AIAA 2003-3568

Impact of Flow Control Technologies on Naval Platforms (Invited)

D. E. Hess and T. C. Fu
Naval Surface Warfare Center
West Bethesda, MD

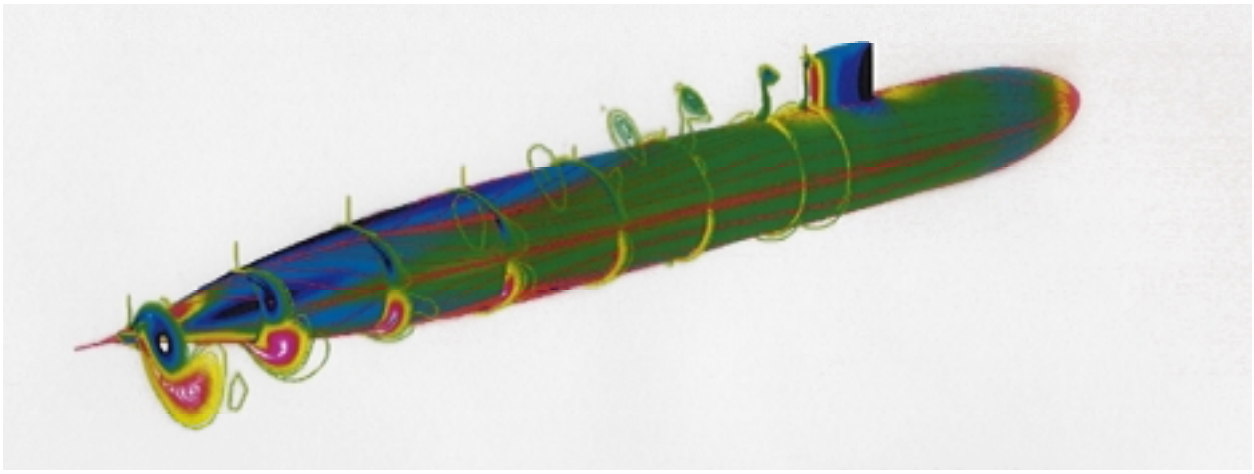

33rd AIAA Fluid Dynamics Conference
23-26 June 2003
Orlando, Florida

IMPACT OF FLOW CONTROL TECHNOLOGIES ON NAVAL PLATFORMS

David E. Hess[†] and Thomas C. Fu[‡]
Naval Surface Warfare Center, West Bethesda, MD 20817

Abstract

This paper highlights flow control technologies and draws a connection between the technologies and US Navy applications, specifically submarines, where possible. This paper does not provide an exhaustive citation listing typical of review papers, but instead focuses on selected applications along with a brief history of submarines. The major theme of the paper is to provide some rationale for which technologies may work in real operational conditions, why technologies have successfully been demonstrated in the laboratory but fail in real operational scenarios, and provide some directions for future research on promising flow control technologies.

1. Introduction

The reader is referred to some overview and review articles[1-5] that go into considerable detail in reviewing the kinds of flow control technologies that have to date been investigated in the laboratory. Further, these articles describe the current physical understanding which explain why such technologies are successful at controlling the flows in question. Beyond the academic success of a technology, benefits/costs analysis projections are sometimes made with that technology for a given application. These analyses (typically conducted by the platform manufacturer) show benefits or cost improvements for a vehicle most often by replacing a current system/sub-system with the flow control system. Although this approach to a benefit/cost analysis is rational, the optimal benefits deriving from the implementation of a flow control system may result from integrating the technology during the conceptual design phase of a new vehicle rather than placement into a current vehicle upgrade. As discussed below for current on-board flow control systems, the integration of the technologies at the design phase is the standard design process. Further, we build on these previous discussions in flow control technology to assess some relative readiness of the technology with respect to the *real* operational issues that may challenge the flow control effectiveness. Factors that influence this readiness level are discussed, and some of the *invisible* barriers that the technology may encounter are outlined when possible.

Flow control methodologies can be classified as passive or active, with the latter requiring power input for the actuator to operate. The actuation system can be steady (e.g., blowing) or unsteady (e.g., oscillatory) and the governing controllers can be open loop (no sensors needed) or closed loop. Technologies that have shown technical success in the laboratory (and often in flight tests) will be discussed, including drag reduction with laminar flow control, riblets, and particle injection for drag reduction and micro-vortex generators and oscillatory excitation for separation control. Other technologies that will be discussed include compliant coatings, circulation control, and thrust vectoring. Some advanced controllers under this discussion include: fuzzy logic, neural networks, and robust and optimal controls. This paper directly expands on the discussion by Joslin, Kunz and Stinebring[1] that focused specifically on aerodynamic to hydrodynamic transition issues without regard to the operational issues as discussed in this paper. As such, some of the implementation examples will pertain to aircraft applications in those cases where the aerodynamic flow control technology is more advanced than for undersea applications.

Before proceeding to the technology discussion, the next section will describe a brief history of submarines with the major milestones, discuss the conventional design process, and outline the operational environments associated with these platforms. Throughout this discussion the reader should understand that some topics are sometimes discontinued or incomplete for classification reasons; however, the goal is to provide sufficient discussion to stimulate research to overcome various obstacles that are noted below.

2. Naval Applications

The discussion will focus on flow control related to submarines and underwater vehicles where possible, although this omits many of the diverse and fascinating aspects of two-phase issues associated with surface ships. As such, this section will highlight the history of the submarine and associated *conventional* flow control technologies that make the submarine a viable platform. Then, the discussion turns to undersea operating issues that would impact future hydromechanic-based flow control technologies as well as scaling issues and laboratory testing.

[†] Member AIAA, Mechanical Engineer, Code 5600
[‡] Mechanical Engineer, Code 5600

2.1 Historical Overview of Submarines

This historical perspective of submarines is derived from a conceptual design text[6] and from the US Department of the Navy Historical Center.[7]

Table 1. History of Submarines.

Date	Event/Name
415 BC	Free Divers – Syracuse
330 BC	Diving Bell – Aristotle
1620 AD	Submersible – Van Drebbly S/M Galley
1776 AD	*Turtle* – David Bushnell (USA); Rev. War
1800 AD	*Nautilus* – Fulton (steam engines)
1864 AD	*Hunley* – US Civil War sank USS Housatonic
1880 AD	Nordenfelt, Gourbet, *Narval* – Laubearf/Holland
1901 AD	*Holland* (SS-1)
1914 AD	U35 Class U-Boats – Germany
1940-50	RADAR, SONAR, Air/water filtration
1955	USS *Nautilus* (SSN 571) - Nuclear

A brief history of submarines is listed in Table 1, with some of the major milestones. Skipping the earlier elements of the history, we focus first on the *Turtle* by David Bushnell as sketched in Fig. 1. In 1776, the *Turtle* was used in the Revolutionary War in a failed attempt to fight the British blockade of the New York harbor. Interestingly, this one-person submarine incorporated a twisted propeller for propulsion and explosives were used as the armament (to be attached to the enemy ship manually).

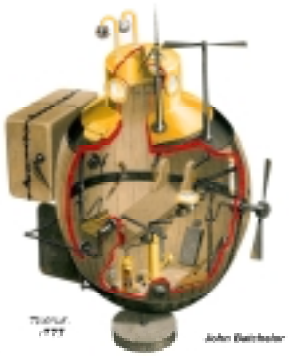

Fig. 1 Sketch of Turtle.[8]

In 1800, Robert Fulton introduced the *Nautilus* submarine, which introduced the steam engine for propulsion. This era also included the introduction of a compressed air system to increase the dive time (4 hrs) and adjustable dive planes for vertical maneuvering. In 1864, H. L. Hunley introduced the *Hunley* as shown in Fig. 2. The *Hunley* was used during the US Civil War and successfully sunk USS *Housatonic*. The 8-person crew served as the propulsion system. Unfortunately, the explosion that sank the *Housatonic* led to the demise of the *Hunley* (and crew).

Introduced by John Holland, the next major milestone occurred in 1901 with the USS Holland (SS 1) becoming the US Navy's first official submarine.

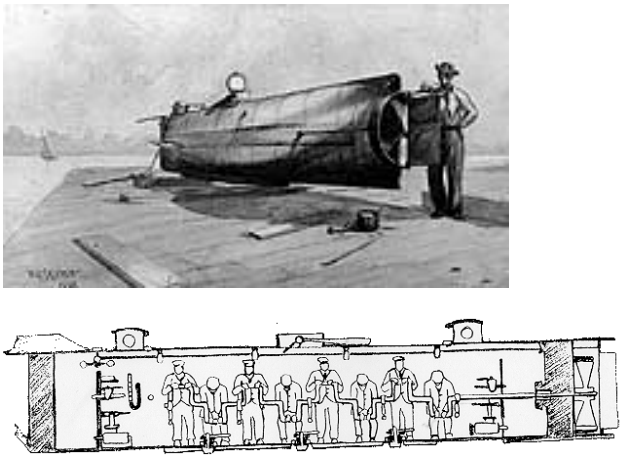

Fig. 2 Sketch of *Hunley*.[7]

Holland's sixth version included a combination of a gasoline engine, batteries, and an electric motor, which combined to serve as the propulsion system. During this same period, Rudolph Diesel introduced the diesel engine, which used a fuel that was more stable and less volatile than gasoline. Diesel engines rapidly became the preference for submarines after the Holland.

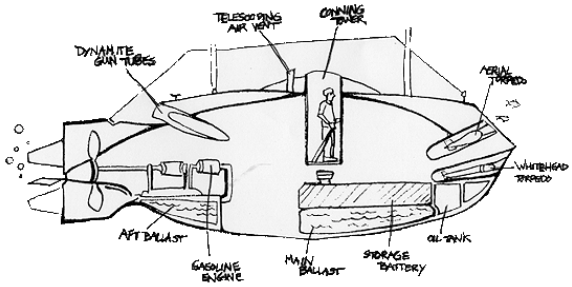

Fig. 3 Sketch of USS *Holland*.[7]

During the 1940-50s, RADAR, SONAR and air/water filtration systems were developed, making the submarine a stealthy and now viable platform for offense/defense. Finally, in 1955 the USS *Nautilus* (SSN 571) was commissioned as the first nuclear powered submarine, developed under the leadership of then Captain Hyman Rickover. The *Nautilus* set undersea endurance, speed, and range records with the now more than 100-person crew.

2.2 Design Considerations

One might predict that a revolution in the design and production of future platforms for the US Department of Defense is imminent, as evidenced by statements taken verbatim from Augustine's Laws.[9]

> *Rule IX: In the year 2054, the entire defense budget will purchase just one tactical aircraft. This aircraft will have to be shared by the Air Force and Navy 3 ½ days each week except for leap year,*

when it will be made available to the Marines for the extra day.

Hence, as budgets decline and costs escalate change must be imminent; however, such change in design comes with great difficulty because the design/production processes have been developed, tested, and molded into the current system over a considerable period of time. Furthermore, cost estimation models rely on historical databases; hence, uncertainty in the cost estimation process may be unacceptable and changes in the design processes would be stifled. Currently, the submarine design process (Fig. 4) begins with the identification of the battlespace scenario and the mission of the future platform based on the scenario.

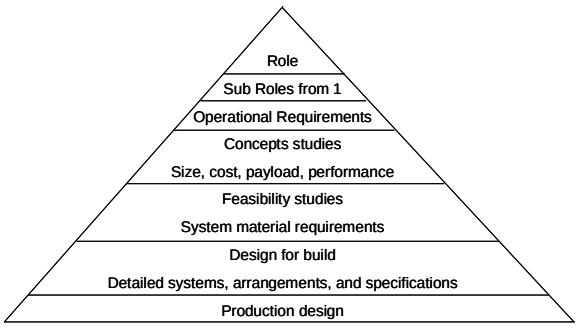

Fig. 4 Submarine design pyramid.[6]

Numerous concept studies that follow, assess the size, payload, performance, and cost of the new concept. Feasibility studies of the most viable concepts are carried further into material requirements and subsystem layout. Ultimately, final and production designs are established followed by the production phase. This process follows a logical progression, with design costs escalating toward the production design. The technologist must clearly understand this process to get a new technology on a real platform. Early in the process, the conceptual designers and feasibility studies would need performance, size, cost, etc. information on this new technology to account for the technology in the design decision process. This clearly assumes that the technology is a hardware component; in a later section on controls, we will highlight advancements in software control methodologies and the more rapid introduction of these techniques into a platform. To close the historical discussion, for Naval platforms, a considerable duration of time elapses between the inception of a flow control concept and the real time use of that concept on the platform. Nevertheless, we will discover that flow control systems have been an integral part of submarines since the days of the *Turtle*.

2.3 Operational Issues

Flow control systems have always been an integral part of submarine design. Rudders and dive planes have appeared on all submarines since Bushnell's *Turtle*, providing vertical and horizontal plane maneuvering capability. World War II submarines added bow-mounted dive planes, which were later replaced by sail planes, only to be later replaced again by bow planes. The latter are now found on Los Angeles class (later versions), Seawolf class and Virginia class submarines. These submarines also added another set of dihedral stern appendages for stability, as well as split dive planes for redundancy.

All of these conventional flow control systems must function not only in the harsh environment of the ocean, as will be discussed in the following section, but must also satisfy the necessary operational requirements for a US Navy submarine. For a system to be included on any US Navy platform, it must be robust for safety assurance. Failure modes are therefore examined, in that system failures must provide for manageable performance degradation. System redundancy is also of paramount importance.

An additional design constraint, which is of primary importance to undersea naval applications and therefore produces a tremendous impact on candidate flow control applications, is stealth. Stealth along with payload capability are high priority requirements for US Navy submarines. Flow control systems must not compromise stealth and must demonstrate benefit over a range of payload displacements. For example, advanced control surfaces, which provide increased maneuverability but also increase flow noise, would not likely be acceptable, nor would, say, a polymer injection drag reduction system that required storing large amounts of polymers.

The challenges of potentially using underwater flow control differ considerably with a classification of the environment. Near the surface, a potential application may have to encounter rain fall, dust, pollution, bird droppings, biological fouling, and wave splash effects. In shallow areas, seawater is typically saturated with oxygen, potentially having a significant impact on corrosive degradation of flow control systems. Corrosion in seawater is a complex phenomena involving salt, debris, chemicals, and living (or decaying) matter; hence, characterizing the effect of this multi-variable issue on a flow control system can be quite challenging. Deeper in the ocean, the oxygen content varies; however, pH is much lower and temperatures approach 0°C. Fig. 5 shows typical water temperature and salinity variations with ocean depth.[10] Underwater flow control systems will have to deal with the large hydrostatic pressures accompanying a

submarine operating at depth, the possibility of biological fouling, and the loads associated with a maneuvering submarine. Finally, near the ocean bottom, bacteria are often present and issues relating to sedimentation may contaminate the flow control system.

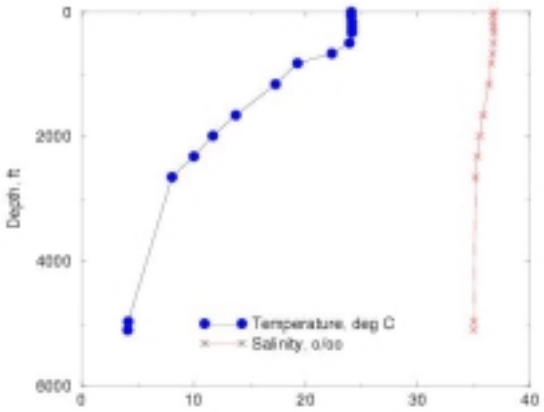

Fig. 5 Atlantic ocean temperature & salinity data.[10]

Additionally, it should be noted that flow control systems are usually first developed and tested as isolated systems at laboratory scales. One of the issues that must be addressed is that most systems are therefore developed and tested at lower Reynolds numbers than that of the full-scale system. Scale effects and efficiencies then become of primary importance. Once a concept has demonstrated effectiveness, its performance can be tested on a radio-controlled model submarine. Depending upon the system, further testing on a quarter-scale submarine model (Large-scale Vehicle, LSV) may be in order before implementation on a full-scale vehicle. This conservative methodical approach allows for the flow control system to be properly tested and characterized and also for the effects of scale to be analyzed and evaluated. Further discussion of scale issues and laboratory testing are found in a subsequent section.

2.4 Air/Water Interface Properties & Seakeeping

The air/water interface presents its own set of challenges. Depending on the design and configuration of a subsystem, flow control devices and systems may have to operate in both air and water. For an underwater platform, the flow control system would be optimized for undersea conditions, but some level of performance may be required in air during free-surface operations. For example, the submarine upper rudders would be in an all-air environment while the submarine is surfaced. If the control surface relied upon submergence for cooling this may be a system issue. As a second example, propulsors may have to consider unsteady loads resulting from partial submergence. Temperature also becomes a factor. MEMS devices must work near 0°C and at high pressures when at depth and must also be functional at one atmosphere and varying surface temperatures when surfaced.

As submarines approach the surface, they generally slow down. This reduces conventional control surface effectiveness because the control surfaces are foil shapes dependent upon speed to generate lift. At shallow depths suction forces from the seaway increase, which can in turn increase vehicle motion. This presents an additional issue, in that flow control systems must operate effectively over a range of speeds and ship attitude (roll, pitch and yaw), sea states and headings. Furthermore, when a submarine is surfaced, the control systems that were primarily designed for control and maneuvering while submerged, must still provide sufficient authority when surfaced.

2.5 Laboratory Testing

Testing of submarine hull designs and selected flow control technologies occurs primarily at the Naval Surface Warfare Center (NSWC), Bethesda, MD, which is one of the Navy's model testing laboratories. Captive (towed) and free-running submarine models (Fig. 6) at approximately 1/20th-scale are tested in this facility.[11-13] An NSWC detachment in Memphis, TN contains the Large Cavitation Channel (LCC),[14] which is one of the largest water tunnels in the world and which was specifically designed for model testing. An NSWC detachment in Bayview, ID operates a fleet of two unmanned, autonomous, large scale vehicles (LSV 1 and 2) in Lake Pend Oreille. LSV2 is shown in Fig. 7. These vehicles are approximately ¼-scale free-running submarine models and provide an intermediate-scale platform between the 1/20-scale models and operations conducted at full scale[15].

In order to properly model submarine behavior at full scale using smaller scale vehicles, care must be taken to match dimensionless parameters. Recall that dimensionless variables tend to arise naturally by rendering the governing equations dimensionless. This process yields the Reynolds (Re) and Froude (Fr) numbers for the incompressible Navier-Stokes equations that govern the motion of the fluid. There are six additional equations of motion to describe the six degree-of-freedom motion of a submarine within this fluid.[16-18]

Fig. 6 NSWC 1/20-Scale radio-controlled free-running submarine model

Fig. 7 ¼-Scale LSV2 *Cutthroat* operated at Lake Pend Oreille, ID

These rigid-body equations express conservation of momentum for the vehicle and detail the forces and moments acting on the vehicle in three dimensions. Submarines are designed such that the center of gravity and the center of buoyancy are at the same longitudinal position, but with the center of gravity vertically displaced below the center of buoyancy.[19] This provides a restoring moment (metacentric moment) to disturbances in pitch and roll essential for hydrostatic stability. This hydrostatic moment is in contrast to hydrodynamic moments developed on the vehicle during its motion. The ratio of the hydrodynamic moment to hydrostatic moment gives rise to a dimensionless variable identical to the Froude number as it expresses the ratio of inertial to gravitational effects acting on the submarine[20]. This Froude number arises naturally when rendering the submarine equations of motion dimensionless. Note that this parameter does not arise from a need to match gravitational effects in the fluid, from gravity waves for example, unless the vehicle is operating near the free surface.

To accurately model the motion of a submarine then, one must match the Froude number, and to accurately capture fluid motions one must also match Reynolds number. However, the history of surface and undersea Naval vessel testing is such that full-scale vehicles are operated in the open ocean in salt water and model scale testing is conducted in large basins of fresh water; consideration of any other fluid for routine model scale testing is impractical. Fluid material parameters such as density (ρ), dynamic viscosity (μ), and hence kinematic viscosity (υ) are quite similar for salt water and fresh water. Therefore, when matching Reynolds and Froude numbers at both scales, one must chiefly rely on the variation in length and velocity scales because the fluid material parameters are nearly the same. With only a variation in length and velocity scales, one cannot match both Reynolds and Froude numbers. This fundamental problem has led to the following compromise. The Froude number is matched to correctly describe the submarine motion. The Reynolds number is maintained as large as practical, but with essentially fully turbulent flow over the hull and appendages. Model scale testing at NSWC is typically at Re $=10^7$, whereas full scale vehicles operate at Re $= 10^9$. The consequence of this two-order-of-magnitude difference is that viscous effects are somewhat greater for the model than they are for the full-scale vehicle. Many of the implications of these *scale effects* for model scale testing are known and accounted for; however, a complete understanding has proven to be elusive and is a subject of continuing investigation. Thus, a successful demonstration of a flow control technology on submarines is typically performed at more than one scale prior to full-scale implementation. Opportunities for testing at full-scale are very limited, typically occurring only during hydrodynamic trials of the vehicle. For this reason, water tunnel testing and the use of the LSV, at an intermediate ¼-scale, are useful additional platforms to examine phenomena that may be attributed to scale effects.

3. Flow Control Technologies

The need for flow control technologies to be transitioned to Naval platforms is high; the following comment from the Office of Naval Research demonstrates one aspect of that need.

> *Modern militaries are conducting operations at speeds high enough that successful intervention by the United States (US) will require the transport of men and materiel from the US to distant trouble spots at speeds greater than ever before. Increases of the required magnitudes cannot be had by simply going to bigger propulsion plants because the rate of fuel consumption would bar achieving long range. Instead, a viable solution requires finding and implementing some means of greatly reducing turbulent friction drag.*[21]

In this section, we highlight the various flow control methodologies that have been demonstrated to work either in the laboratory, on a test aircraft or on a naval configuration, but have not yet been accepted on a planned production platform. These technologies include performance improving methodologies such as vortex and separation control and resistance (drag) reduction with methodologies such as natural laminar flow, laminar flow control, bubble/polymer injection, spanwise wall oscillations, compliant walls, riblets, large-eddy breakup devices, and circulation control. In light of the operational issues, this section will provide some insights into inherent inhibitors that must be overcome to reach the platform (with the desire to foster innovation in the community).

Before proceeding mention should be made of the tremendous 414-page tome produced by Wilson and von Kerczek[22] in 1979 on the topic of force producers for use in marine vehicle control. They survey concepts, describe how each device operates and describe the forces that are attainable. They provide some guidance on those devices most likely to be of use in the immediate future.

3.1 Natural Laminar Flow

Essentially, the motivation for achieving laminar flow can be explained by examining the contributions to the drag.[23-24] Friction drag contributes a large portion of the overall drag. Because laminar flow has considerably less friction drag than turbulent flow, maintaining laminar flow through natural active means can benefit an aircraft, submarine, etc.

Natural laminar flow can be achieved if the hydrodynamic shape is designed to have a favorable pressure gradient to delay transition. This technique has been demonstrated to be a viable method to achieve laminar flow in water on bodies of revolution tested in a water tunnel[25-26] and in a water towing tank,[27] as well as for a flat plate model.[28] These results have clearly showed regions of laminar flow. These demonstrations suggest that achieving laminar flow in water is possible albeit there may be some implementation issues which will inhibit laminar-flow configurations from reaching fruition. For example, a torpedo designed to achieve laminar flow may alter the length of the weapon such that it no longer fits in the rack (& tube) of a submarine. Thus, operational limitations and not technical feasibility could inhibit the laminar design. However, because laminar flow is extremely sensitive to disturbances, the main inhibitor may well be debris in the ocean or contamination on a surface, causing the *laboratory laminar model* to become turbulent in the *real* environment. There is no evidence that natural laminar flow concepts will work in an ocean environment.

3.2 Laminar Flow Control

Laminar flow control (LFC) is an active boundary-layer flow control technique employed to maintain the laminar flow at Reynolds numbers beyond those which are normally characterized as being transitional or turbulent in the absence of control. The concept is referred to as active because energy input is required to obtain resistance reduction; hence, energy input/output balances must be considered to assess the impact of the control approach on the prototype.

The majority of laminar flow control activities in air have been associated with the use of suction through porous, perforated, or slot surfaces. In air, small amounts of suction delay the onset of transition by changing the curvature of the velocity profile in such a manner as to make the profiles more stable. Suction systems become, for the most part, impractical in sea water due to the rich variety of particulate the system would have to encounter. In addition, various microorganisms (e.g., plankton) would presumably overwhelm the suction system making the technology non-functional in the real operating environment of the ocean unless some thought was devoted to a practical filtration system.

Whereas active cooling can delay transition in air, underwater research and applications have focused on achieving laminar flow through active heating control. Because viscosity decreases with increased temperature for water, the heating works to cause the velocity gradient near the wall to increase and become more stable. For example, Strazisar et al.[28] forced periodic disturbances in a heated flat plate boundary layer. The results showed that Tollmien-Schlichting instabilities had decreased growth rates with the use of heating and that nonparallel effects were important near the critical Reynolds number. As with a natural laminar flow system, the boundary layer would contain various forms of particulate. Also, the energy input/output assessment of efficiency may rule out this technology. From stealth requirements, heat into the flow may induce a detectable signature that would be unacceptable and therefore prevent a proven flow control technology from reaching an undersea application.

3.3 Polymer/Particle/Bubble Injection

Associated with turbulent drag reduction, random-coiling macromolecules, polyelectrolytes, surfactants, and fibers have been tested primarily in pipes.[29] It is sufficient to note that the different properties of the additives impact the resulting turbulent flow and subsequent performance benefits.

Hoyer and Gyr[30] summarized the concept of drag reduction in turbulent pipes by heterogeneous polymer injection. Heterogeneous drag reduction involves

polymer injection into the shear flow, which only affects the near-wall region such that the core flow remains Newtonian. They note that drag reduction occurs at a certain onset value (critical shear stress) and is limited by an asymptotic value.[31-32] A rather good historical perspective is given on the subject along with summarized trends in the velocity fluctuations, power spectra, averaged time between bursts (which incidentally increased in drag reduced flows); however, the precise explanation for how this polymer/turbulence interaction leads to drag reduction is, as yet, elusive.

Similar to polymer usage, the employment of bubbles into the near-wall region of a flow has a goal of drag reduction (through reduced skin friction). This two-phase flow in a boundary layer leads to less resistance[33] and therefore a drag reduction. There has been quite a significant body of research in this area to make it technically feasible. A good discussion of aspects of bubble injection was given by Meng and Uhlman.[34] Of note, the ratio of injection velocity to external flow velocity impacts the bubble size and formation, where the smaller the bubble, the more likely the bubble will remain near the wall. Also, Madavan et al.[35] looked at the impact of different porous materials on drag reduction with microbubbles. Although they found that the material was not important, the amount of porosity for different flow speeds did affect the resulting drag. Larger pore size and smaller surface area performed better for low speed flows, whereas at higher speeds smaller pore sized materials led to better skin friction reductions.

Fontaine and Deutsch[36] have looked at the effectiveness of 5 different gases for microbubble drag reduction. They concluded that the type of gas is largely immaterial (all are effective), and that the greatest correlation to drag reduction was the volume flow rate of the gas and the location of the bubbles in the boundary layer.

While experiments have for some time been successful in reporting drag reduction with the use of microbubbles, Xu, et al.[37] have recently reported success in demonstrating drag reduction by seeding the boundary layer of a turbulent channel flow with microbubbles within a direct numerical simulation. Bubbles introduced into the boundary layer in planar layers at average volume fractions up to 8% for a Reynolds number, $\mathrm{Re}_* = 135$, and for dimensionless bubble radii of $a^+ = 13.5 - 40.5$, show drag reductions in the range of 0.5-8.5%. A key finding is that "the strongest, sustained reduction in drag is achieved for the small bubbles, $a^+ = 13.5$, …"

Reinforcing the latter comment are earlier remarks by Merkle and Deutsch[38] where they note that "smaller bubble sizes would be expected to be more stable to coalescence and would slow growth rate giving longer regions of persistence of C_f reduction, but methods for controlling bubble size are not available". Microbubble addition with conventional porous plates has been shown to dramatically reduce friction drag. The large amounts of gas-flux typically necessary for this drag reduction have made the technique difficult and impractical to apply to full-scale naval vessels and torpedoes. However, the efficiency of such systems can be dramatically increased if the gas flux is only devoted to producing the bubbles that are small enough to be effective for drag reduction.[39] Recent investigations at the Univ. of Illinois[40-41] have focused efforts on producing microbubbles with diameters of $50\mu m$ or less electrolytically using MEMS-based microbubble generators. The microbubble generator is realized using surface micromachining technology, and the bubble generation sites are defined using photolithography. The appeal of such a technique for use on Naval vehicles lies in the *absence of the need* for carrying gas onboard, for providing the requisite pumping and plumbing and for porous plates or injectors.

Research in polymer/bubble drag reduction has continued in the US under a DARPA Friction Drag Reduction Program and in Japan. (A review of recent Japanese microbubble work may be found in Kodama, et al.[42]) Both programs have focused on understanding the physics of the polymer/turbulence and bubble/turbulence interaction through theory and modeling.

For polymers, the modeling has focused on Brownian dynamics through RANS/turbulence modeling efforts. The most important of the missing components for identifying cause-effect relationships for the drag reduction involves the linkage between molecular properties and the modeling/viscoelastic experiments. Ultimately, the drag reduction system should be designed from the molecular level. The rationale for this point results from evaluating the types of polymers used for drag reduction. It is our view that the system requirements for a real platform are faulted by our inability to design a very high-weight polymer that can be *easily* prepared for injection into the near-wall boundary layer and lead to drag reduction. At this point, there is no question that drag reduction is possible. The real question becomes: *Can a system be designed that buys its way onto the platform?* This is a considerable challenge unless we can design the needed polymer attributes.

For bubbles, the concept becomes impractical for undersea vehicles operating at large depths from an energy input/output assessment; however, bubbles

employed for surface ship drag reduction or smaller underwater vehicles operating in littoral regions may soon become a viable concept.

3.4 Wall Oscillations

A number of studies have been carried out to determine the impact of oscillations on turbulent drag. Choi and Clayton[43-44] showed, through wind-tunnel experiments, that spanwise oscillations of a wall led to a 45% reduction in the skin friction of a turbulent boundary layer. The study was conducted at a Reynolds number of 1190 based on momentum thickness and with a moving wall frequency of 5 Hz. An analysis by Dhanak and Si[45] suggested that the reduction in skin friction and Reynolds stress on the oscillatory wall is assocated with an *annihilation* of the low speed streaks. An alternate means to achieve flow oscillations near a wall is by using unsteady suction and blowing. Tardu[46] observed a drag reduction by using time-periodic blowing through a slot of a flat plate in a wind tunnel. Just downstream of the slot, the near wall region was reported to be relaminarized during the accelerated phase of the actuation.

Although wall oscillations tend to reduce skin friction levels, implementation issues similar to those for LFC may prevent the technology from being viable for undersea applications.

3.5 Lorentz Force Actuation

The interaction of an electric field, characterized by current density, **j**, with a magnetic field, **B** in a conducting fluid gives rise to a body force, $\mathbf{j}\times\mathbf{B}$, which acts in a direction normal to both **j** and **B.** Furthermore, varying the electric field will in turn vary the applied body force. According to Bandyopadhyay, et al.[47], the fact that this force could be used to pump fluid was experimentally demonstrated as early as 1832 by Ritchie[48]. Because of the conductive nature of seawater, the use of the Lorentz force to alter boundary layer properties and thereby reduce drag on a vessel moving through a viscous conducting fluid is an attractive concept for naval applications. This field has recently been reenergized with a series of simulations and experiments. These works have directed the body force within the boundary layer longitudinally to accelerate or decelerate the flow, in the spanwise direction and normal to the flow. A good review of recent work may be found in Berger, et al.[49]

The latter paper performed a direct numerical simulation of low Reynolds number turbulent channel flow with an open-loop spanwise oscillating Lorentz force applied. They found that skin friction drag could be reduced by 40% for $\mathrm{Re}_\tau = 100$. The efficiency of the control method, defined as the amount of power saved due to drag reduction divided by the power required to produce the Lorentz force, was found to be poor. Namely, the power used was estimated to be three orders of magnitude larger than the power saved. Further, they found that for increasing Reynolds number, drag reductions were smaller, and the efficiency was even worse. They also investigated a closed-loop scheme, which directed a wall-normal Lorentz force to oppose the wall-normal velocity component close to the wall. The behavior of the latter velocity component was inferred from the local spanwise shear stress at the wall. This method was found to give similar levels of drag reduction with a much better efficiency, 0.167 compared to 0.001.

Park, et al.,[50] have performed an experimental verification of the previous work using an open-loop temporally oscillating spanwise Lorentz force created by embedding magnets and electrodes in the wall of a turbulent salt water channel flow. They have reported consistent drag reductions (by the direct measurement of drag) of 9% for $\mathrm{Re}_* = 290 \text{ and } 400$. Early results confirm that the efficiency is poor; however, the experiments at Brown are continuing as of this writing. Details of the actuators and their performance will soon appear in Park, et al.[51].

Jaskolski[52] has also performed an experimental implementation of open-loop temporally oscillating spanwise Lorentz force actuation in the MIT Marine Hydrodynamics water tunnel. Drag reductions of 25% to 37% at higher Reynolds numbers than the previous work, inferred from measurement of the velocity gradient at the wall, were reported. Although he also reported a low efficiency, 0.015 at a speed of 3 m/s, he found that input power varied inversely to flow speed. This raises the tantalizing prospect that at a high enough flow speed, 8.2 m/s was estimated, a break-even point would be reached with efficiencies greater than one above this critical velocity. Work continues at MIT as of this writing.

Du and Karniadakis[53-54] and Karniadakis and Choi[55] discuss direct numerical simulations of a turbulent channel flow that demonstrate that the use of a transverse traveling wave can be used to achieve significant drag reductions, 15-30% at $\mathrm{Re}_\tau = 150$. The simulations show a modification of near-wall streaks as opposed to the interaction generated by an oscillating Stokes layer. They suggest that the traveling wave can be created using Lorentz force actuation. Furthermore, their calculations estimate an efficiency of 5 when used open-loop with a complex multiphase pulsing pattern.

Finally, Bandyopadhyay, et al.[47] review recent work in this area, conduct a DNS supplemented by a low Reynolds number channel flow visualization experiment, and then perform a higher Reynolds

number experiment ($\mathrm{Re}_\theta > 2300$) on an axisymmetric body. Open-loop temporally oscillating wall-normal Lorentz force actuation is employed using an array of microtiles. The experiment was carried out in the Naval Undersea Warfare Center (NUWC) stainless-steel salt water tunnel. They report no clear evidence of drag reduction using a drag balance; however, mean velocity and wall-normal turbulence intensity measurements suggest that a weak drag-reducing effect is present.

These investigations demonstrate the encouraging news that some degree of drag reduction using Lorentz force actuation is possible. However, this is tempered by the sobering reports of very poor efficiency. We believe that there are some naval applications where drag reduction, at even a high cost, could serve as a *mission-enabler*, such that efficiencies greater than one would not necessarily be required. Without an improvement in the current state of affairs, with efficiencies several magnitudes lower, implementation is unlikely. Because Lorentz force actuation is quiet, its intermittent use for separation control or vortex mitigation might prove to be attractive avenues for exploration.

3.6 Compliant Walls

Compliant coating research began with the hypothesis that dolphins achieved very high speeds through a natural drag reduction mechanism brought about by means of their compliant skins. As such, most of the research in this area has used this argument as a basis for their work. This attempt to link nature's wonders with engineering design has always existed in science; however, in the research environment of the late 1990's the new term *biomimetic* has arisen to signify this scientific reasoning.

The linkage between the dolphin and compliant coatings arose from what is termed "Gray's Paradox." Gray[56] compared the resistance of a towed rigid body and the observed speeds of a dolphin to suggest that the dolphin's muscles must be able to generate energy at a rate seven times greater than any other mammal to attain the recorded speeds. Fein[57] has performed a rather substantial review of the issues (i.e., claims) of researchers associated with linking dolphin dynamics to compliant coatings to drag reduction. Fein concluded that Gray's Paradox was built on incorrect data and that there is no reason to believe that friction drag reduction and the dolphin's motion are related. However, Fein suggests that some form of wave or form drag reduction may be possible for dolphin-like animals.

In the early 1980's, Carpenter and Garrad[58-59] showed theoretically that Kramer-type surfaces could lead to potential delays in transition by suppressing the amplification of Tollmien-Schlichting instabilities. Further, they indicated deficiencies in previous investigations which may have prevented achieving results comparable to those of Kramer.

Experiments performed by Willis[60] and Gaster[61] showed favorable results using compliant walls. The research of Carpenter[62] suggests that Tollmien-Schlichting dominated transition can be postponed to very high Reynolds numbers using multiple compliant coating panels. As an example, Carpenter shows that the concept of maintaining laminar flow via compliant coatings appears to be most promising for applications such as hydrofoils and torpedoes, where the estimated skin-friction drag reductions are 83% and 19%, respectively. A recent review concerning progress towards making the use of compliant walls a practical method of laminar flow control is provided by Carpenter, et al.[63] For a submarine, no estimated benefit can be predicted. Obviously, the submarine would be a very exciting application for compliant coatings if turbulent drag reduction were feasible. However, as stated before maintaining laminar flow in the real ocean where contaminants abound is unlikely.

The fluid-solid interaction problem for drag reduction in turbulent flows is much more challenging and less understood compared with the above discussed laminar flow application. Whereas a few potential (albeit competing) modes are possible in laminar flows, the infinite dimensional problem exists for turbulent flows. Interest turned toward the use of compliant walls for turbulent drag reduction in the late 1970's and 1980's when NASA[64] and the Office of Naval Research[65] sponsored investigations involving the use of compliant walls for the turbulent problem. Although most of the results from this era were either inconclusive or unsatisfactory, the contributions, together with earlier results, have acted as stepping stones to the understanding of the physically complex fluid/wall interaction phenomena. More recently, Duncan[66] has simplified the infinite dimensional system by assuming that a superposition of a convecting pressure pulse on a potential flow could represent a bursting event. The coating then responds to the pulse depending on the speed of the pulse. As the flow becomes high speed, unstable waves develop on the coating. Such compliant coating disturbances have been documented in previous experiments.[67]

A series of experimental investigations examining the interaction of a passive compliant surface beneath a fully developed turbulent boundary layer on a flat plate was conducted by Hess[68-70] in the early 1990's as a result of the aforementioned ONR research initiative. These experiments were designed to probe the fluid-structure interaction rather than represent another drag reduction attempt. The work used a laser-based

displacement gage[71] to measure the vertical component of displacement (δ) of the compliant surface while two components of velocity in the buffer layer were simultaneously recorded using an X hot-film probe. A range of compliant surface material properties was tested using cured mixtures of silicone elastomer and silicone oil. In every case the Reynolds number of the flow was controlled to keep the fluid-structure interaction in a range of small amplitude stable disturbances and to avoid the unstable static divergence waves known to increase drag. A photograph showing an example of the interaction is found in Fig. 8.

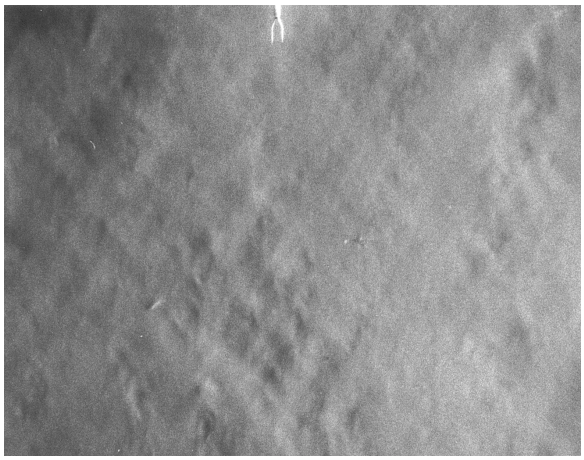

Fig. 8 Stable displacements of a compliant surface beneath a turbulent boundary layer. The image size is 13 cm x 17 cm.

The variable-interval time average (VITA) technique of Blackwelder and Kaplan[72] was employed to isolate bursting events in the velocity time histories and local conditional averaging was used to discover the displacement response of the compliant surface during these bursting events. The compliant wall tended to augment fluid motion normal to the wall, and the signs of u and δ were typically opposite. These results combined to cause increases in Reynolds shear stress. The conclusion was that the wall stress field resulting from near wall bursting events induced displacements in the compliant wall and these displacements then effected changes in the velocity field primarily in the normal velocity component. The phase of the displacement fluctuations relative to the velocity fluctuation profiles during bursting events was ill suited for reductions in Reynolds stress below levels found for a rigid wall. However, the data did show that motion of the surface beneath a turbulent boundary layer can exact significant changes in near wall structures suggesting that active or smart wall actuation may provide positive results.

Indeed, that is the case as demonstrated by Rathnasingham and Breuer[73-74] where they successfully applied a linear feed-forward control algorithm using upstream wall-based sensors and a down stream actuator in a turbulent boundary layer. They demonstrated reductions in streamwise velocity fluctuations, wall pressure fluctuations and mean wall shear stress. Further discussion of this topic is postponed to the section on Control Methodologies.

3.7 Riblets

Pioneering research in riblet technology occurred when Walsh[75] reported an 8% drag reduction (for a zero pressure gradient, turbulent flow over flat plate configuration) was demonstrated using two different kinds of riblets. Numerous wind tunnel experiments[76-77] were conducted on a variety of riblet shapes, sizes and spacing to maximize the drag reduction. They found a maximum repeatable drag reduction of 8% for a symmetric v-groove riblet and a sharp peak-concave valley riblet both sized and spaced on the order of 10-16 wall units. However, consistent drag reductions were noted for riblets sized and spaced on the order of 25-30 wall units.

Gallagher and Thomas[78] used v-groove riblets on a flat plate in a water tunnel and found no net drag reduction, although the near wall region of the flow difference compared with that for a smooth flat plate. A notable accomplishment was the use of riblets on America's cup winner Stars and Stripes.[79-80]

3.8 Vortex and Separation Control

Vortex generators (VG) are passive or active devices used to induce a vortex and thereby inject a localized low-pressure region. The need for this vortex is generally associated with an otherwise separated flow, which causes severe performance penalties. Large vortex generators have been used on the aft portion of an aircraft to improve the overall performance of the aircraft. Vortex generators have been tested on the after-body of a C-130 aircraft model to postpone separation.[81] The after-body of this configuration has a highly adverse pressure gradient and hence separation control would be beneficial to the aircraft. Results from tests of numerous placements of the vortex generators led to reduced drag compared with the baseline configuration. A similar study[82] with Boeing 747 and Lockheed C-5 aircraft models led to total drag reductions of 1% and 2%, respectively, for these configurations. Lin[83] and Lin et al.[84] have shown that using micro vortex generators (MVG) on the flap of a high lift system can mitigate flow separation, leading to a 10% increase in lift and 50% reduction in drag. Together this leads to over a 100% increase in L/D. For the conventional high-lift system, the MVGs would be

hidden during cruise conditions. Hence, there would be no drag penalty during cruise.

Unlike the aircraft application that focused on *correcting* a separation issue, micro-vortex generators have also been used by Lin, et al.[85] on a submarine radio-controlled model (RCM) to alter the crossflow around the submarine and improve maneuvering. Typically, when a submarine makes a hard turn, vorticity, which is shed from the upstream appendages (particularly the sail), interacts with cross flow about the hull. The net effect of this complex interaction is undesirable pitch and depth changes (rise or dive) that accompany the turn. This work examined 19 configurations of MVGs that varied in number and placement. The optimal configuration was a set of 6 MVGs placed along the deck of the submarine in alignment with the sail. The small number of devices as well as their location also conveniently minimized the device drag penalty for straight-ahead motion. The MVGs significantly reduced the tendency of the submarine to dive, and resulted in a 20% reduction in turning diameter for equivalent depth excursion. Furthermore, the time required to complete the turn was reduced by 13%. Reductions in pitch and roll were recorded as well.

Of course the VG is a passive technique and can have obvious implementation limitations. Ideally, "pop-up" and on-demand VGs are desirable but are probably unaffordable for this platform. Significant effort is still required to (experimentally) determine where the VGs should be positioned and what size or shape of VG is required for a given application. No correlation tools exist for the design or use of the VGs; however, a simple model of the device does exist for computational modeling of the induced effects of the VG on a given flow.[86] A good experimental database is needed to better develop micro-VG models for CFD.

During maneuvering of a submersible vehicle, crossflow separation often leads to undesirable forces and moments. Wetzel and Simpson[87] investigated the use of vortex generators (passive) and directed jets to control the separation process and mitigate the forces. Through oil flow visualization and force and moment measurements, the results indicated that yaw moment and normal forces could be reduced as much as 35-50% and axial and pitching moments changed by 300% using vortex generators. The jets were ineffective in altering the forces and moments for this study.

One type of actuator consists of an angled orifice through which oscillatory pulses of fluid are injected. The angular injection causes streamwise co-rotating vortices to be produced in the flow. The vortices can cause an otherwise separated flow to become attached, thus leading to improvements in aerodynamic performance. This actuation technique is referred to as pulsed vortex generators (PVGs).[88] This actuation technique works well at high angles of attack, but is essentially ineffective at low angles of attack where separation is typically not a problem.

Some of the earliest research in zero-net-mass actuators began in the 1950's with the acoustical streaming around orifices by Ingard and Labate.[89] Their results showed four flow field regions which were a function of the driver frequency. The regions characterized the different observed flows emitted from the orifice. The results suggest a maximum velocity of 7 m/s was achievable with this early zero-net-mass actuator.

Recent studies[90-91] have demonstrated the use of micro-sized piezoelectric actuators for flow manipulation. The proposed piezoelectric actuator has a net mass flow of zero; however, peculiar to this type of actuator is the resulting jet-like flow fields, which can emerge with actuation. Hence, this kind of device has been referred to as a synthetic jet.[92] Actuators of this type have been shown to generate velocities from a fraction of a meter per second to tens of meters per second and over frequencies ranging in the kilohertz. Progress has been made in modeling, designing, and building synthetic jet actuators.[93-95] With further validation, the zero-net-mass jets may potentially lead to aerodynamic performance benefits through enhanced lift on wings, drag reduction during cruise through advanced active Laminar Flow Control (LFC), and on-demand control moments, thereby eliminating or reducing traditional flap/slat hardware.

One major obstacle, which must be overcome with the synthetic jet technology, is associated with the significant noise source introduced by operating these devices at a resonant condition (which is the condition of maximum induced jet velocity). Either limiting the operation of these devices to non-resonant conditions or using some form of noise control are potential means to overcome the obstacle. Finally, the mass flux from the current generation of devices is insufficient for most full scale applications; however, potential stacking of the actuators may overcome this deficiency.

Piezoelectric actuators[96] and leading-edge flaps[97] have been used in a manner similar to active vortex generators to control flow separation. Notable improvements in performance were measured, with the peak effectiveness of the actuator occurring at a frequency near the natural shedding frequency of vortices in the shear layer.

Separation control on a two-dimensional airfoil at angle-of-attack has been demonstrated in low and high Reynolds number wind-tunnel experiments by the introduction of a periodic momentum flux through a

slot opening in the model.[98-102] Although an oscillatory blowing valve was used to generate the periodic disturbance, any type of actuator having similar performance characteristic could have been used. A dimensionless momentum coefficient and a frequency characterized the actuator-induced response, where the distance between the separation point (with no control) and the trailing edge is used as the characteristic length scale for nondimensionalization. An oscillatory blowing valve was chosen because of the ease with which a steady disturbance, oscillatory disturbance, or superposition of steady and oscillatory disturbances could be generated. This technique was effective because it promoted mixing between the higher momentum fluid above the otherwise separated region and the lower momentum fluid at the surface. The enhanced mixing brings the higher momentum fluid close to the surface making the boundary layer more resistant to separation. This active means of control has the advantage of eliminating or reducing separation without the performance degradation at off-design conditions associated with passive control. Also, the periodic control is two orders of magnitude more efficient than steady suction or blowing traditionally used for separation control.

3.9 Circulation Control

Development of circulation control (CC) was initiated in England in the 1960's[103-105] and was identified by NSWC a few years later as a promising technology for application to Naval aviation, especially rotorcraft but also for fixed-wing aircraft[106]. At about the same time, the Office of Naval Research funded West Virginia University (WVU) to investigate the theoretical and experimental aspects of circulation control by blowing.[107] In 1974, WVU flew a light aircraft that had been modified to have CC wings.[108] Development for both rotary-wing and other fixed-wing configurations continued at NSWC through 1990, and sporadically since then, within the Aerodynamics Department.

In 1973, Lee, et al.[109] examined the use of rotating cylinders in conjunction with a lifting surface to increase lift or delay stall. Their investigations were targeted towards submarine control at slow speeds. They felt that the concept had substantial potential, but that further experimentation was warranted.

Elsewhere, CC on a wing has been investigated to generate increased lift coefficients.[110-112] Via engine bleed, air is blown through a slot on the upper wing surface, just upstream of the rounded trailing edge. This blowing increased the lift by several times compared to a conventional passive flap system. The application of circulation control technology to both lifting and control surfaces has the potential to provide improvements in performance and operational capabilities of both commercial and military aircraft. These significant potential benefits have been derived primarily from component studies on unswept airfoils. A recent review of circulation control work may be found in Englar.[113]

An alternate to steady blowing for circulation control might entail the use of unsteady blowing in an attempt to reduce the amount of energy requirements to the control system. As such, separation control by unsteady tangential blowing over the flap of a wing/flap model was compared with steady blowing control.[114] The experiments suggested that a significant reduction in the amount of mass flow could be realized through unsteady blowing. As the pulsed frequency increased up to 60 Hz, the lift increased. Beyond 60 Hz, little or no gain in performance was measured.

There are now both military and commercial applications to production aircraft, where the benefits obtained were noise reduction (on the NOTAR helicopter line[115]) and reduced cost of manufacture (on the Navy V-22 aircraft[116]). Another interesting application involves a wind tunnel at MIT that uses two non-moving lifting surfaces in the test section to generate simulated wind gusts.[117] The gusts are produced by cyclic modulation of dual-slotted Coanda trailing edge blowing, in the same manner as could be used for the control surface of an underwater vehicle.

Thus, the ability of a wall jet emitted from a tangential slot to follow a curved surface (the Coanda effect[118]) is a flow control technique under continued development at NSWC. Through a momentum exchange with the upstream flow, the Coanda wall jet directed over a rounded trailing edge of a planar surface changes the relative momentum levels of upper/lower surface flows thereby shifting the location of the merging flows and hence the wake formation point. Large increases in lift coefficient result, well beyond that available from conventional surfaces. Although this technique is basically that of boundary layer control, it is commonly referred to as circulation control. Effectively, the rear stagnation point is moved (the leading edge stagnation point also moves in concert). Gain, or augmentation ratio – defined as the ratio of lift force developed to the jet momentum force – of up to 90 has been found for CC airfoils.[119] The attractiveness, in addition to substantial force augmentation, is that the lift can be modulated by simply controlling the flow through the slot. A further advantage is that the coefficient of lift becomes larger as free stream velocity decreases for a given slot flow pumping power. This inverse relationship with speed makes CC particularly attractive for low-speed applications where conventional control surfaces begin to lose effectiveness.

A Coanda wall jet technique for CC was implemented by a team at NSWCCD on a very low aspect ratio wing in the Navy's Large Cavitation Channel (LCC) in order to demonstrate the potential for undersea (particular submarine) use as a control surface.[120] The test was very successful and showed substantial force augmentation in a variety of modes of implementation. A cross-sectional view showing the Coanda trailing edge is depicted in Fig. 9 (top) and a view of the wing mounted in the test section of the LCC is shown in Fig. 9 (bottom). A paper documenting the work and the results for this recently concluded test is under preparation as of this writing.

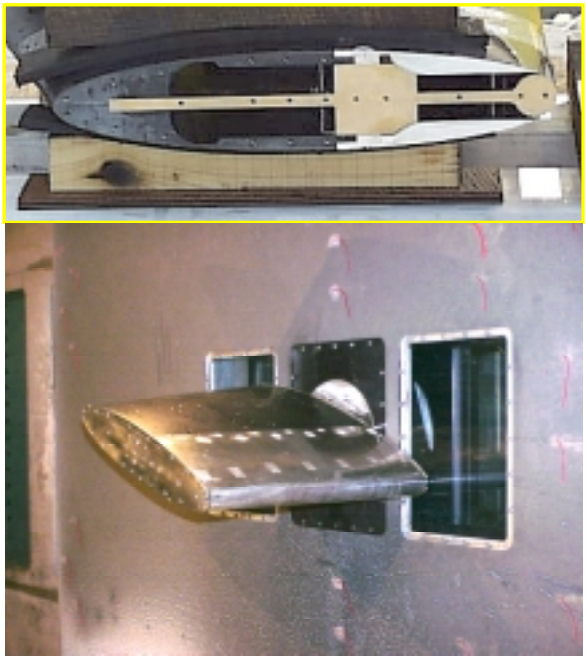

Fig. 9 (Top) Cross-section of NSWC CC wing (resting in packing material)
(Bottom) CC wing mounted in LCC test section

The physical implementation of the Coanda wall jet form of circulation control is recognized by the incorporation of a slot just upstream of a rounded trailing edge whose radius is similar to that used for wing leading edges. Slot flow control feedback for closed-loop control of such a system could be implemented with pressure or flow rate sensors. Alternatively, using the fact that loads on a CC surface have been shown to be linearly related to the pressure difference between two surface pressure taps[121], one could indirectly sense generated forces. These taps are located at the center on each side of the foil; this method works well in the absence of massive flow separation.

Of concern for the potential implementation of CC on submarines are such issues as: acoustics, slot fouling from marine growth, early and potentially disruptive cavitation due to Coanda surface suction, and the effect of short span (low aspect ratio). The LCC test referred to above demonstrated that the last two issues were not a problem[120]. The acoustics concern essentially depends upon whether the flow exiting the slot is laminar or turbulent on a full-scale design.[122] Finally, slot-fouling effects have not been investigated thoroughly and remain a subject for future examination.

3.10 Fore-body Control

For bodies of revolution at high angle-of-attack, side forces appear in the nose or fore-body region with sufficient intensity that control surfaces may be rendered inadequate to control the body. With fighter-type aircraft at high angle of attack, the conventional control surfaces may become ineffective with the onset of fore-body yawing moment forces. An active control system is desired which can serve to eliminate the unwanted forces and impose desirable forces (control).

Fore-body control is a complicated technical challenge. Any potential asymmetries in the nose geometry can be sufficient to cause asymmetric vortices. Nose slenderness becomes an issue as well. For example, Ericsson and Beyers[123] discussed the comparison of using fore-body control on a fighter versus a high-speed transport type aircraft (slender nose). The analysis suggested that the relation between the blowing rate and moment could be characterized as linear at low angles of attack and nonlinear at modest angles of attack. Further, very low rates of blowing could cause an asymmetric vorticity field, which implies that commercial manufacturing tolerances may (depending on the configuration) have to be stringent, and this may make the flow control technology un-economical to commercial customers.

Simple bodies of revolution through full configuration models have been tested with various control strategies, including strakes and surface jet and slot blowing. Nose strakes can be used (if strategically placed) to control the magnitude and direction of the forces associated with the vorticity. The blowing technique was most effective when the blowing was implemented near the dominant vortex and directed downstream. The blowing could effectively switch the sign of the yawing moment and was a function of the mass flow coefficient. Fore-body blowing on a slender cone suggested a preferred injection of fluid normal to the geometric surface; however, this preference changes with the objective of the control. Blowing through a slot near the nose is effective for controlling the vorticity field at a lower angle of attack compared with blowing through an orifice. Suction through a slot was

noted to be effective if the slot was located very near the apex of the nose. Suction through orifices is effective in controlling the asymmetric forces at high angle of attack and appears to be a function of flow rate rather than mass flow coefficient. Finally, moving strakes were investigated in wind tunnel experiments. Although equivalent authority can be gained with a single nose strake, the rotatable strakes can vary the asymmetric vortex field. The level of forcible symmetry or asymmetry with rotatable strakes is a function of the angle of attack.

This flow control technology was included for the sake of completeness. It is relevant to naval aircraft, but no undersea applications are envisioned at this time.

3.11 Wake Drag Reduction

Acoustic feedback approaches are an alternative means for wake control unlike the large-scale active vorticity control schemes discussed previously. Ffowcs-Williams and Zhao[124] exploited the well-established susceptibility of von Karman vortex streets to sound using a feedback control scheme. In their research, a loudspeaker was mounted downstream of a circular cylinder at Re=400. Feedback from hot wire sensors mounted in the cylinder wake provided input to a control system that operated in a band about the main vortex shedding frequency. Wake velocity fluctuations were suppressed at the nominal dominant shedding frequency of the cylinder by as much as 30 decibels. So the approach taken is to impose stability on the natural system such that the exponential growth is suppressed. This contrasts with the approaches of previous sections, that attempt to exploit or *program*[125] the inevitable large-scale structures that dominate high Reynolds number separated flows rather than attempt to suppress them.

3.12 Advanced Control Surfaces

Water tunnel testing at 1/16-scale[126] and computational work,[127-128] both sponsored by the Office of Naval Research (ONR), have validated an advanced sternplane concept for submarines. The design alters the circulation about the foil by adding a small independently actuated hinged tab at the trailing edge of the flap (primary control surface). The tab was 10% of the mean chord of the overall appendage, including the stabilizer. This Tab-Assisted Control (TAC) design has the potential for lift enhancement at low speeds, torque reduction at medium speeds, precision control at high speeds, lift reduction in the event of a jam in the primary control surface and for back-driving the flap. Tabs have been used for many years in the aviation industry to reduce flap torque and for fine control. For marine applications, flaps must be well balanced to prevent tremendous torque requirements for flap actuation. Furthermore, for submarine applications, housing the tab actuation system in the flap is desirable.

This presents significant challenges for conventional actuation in the limited volume of the flap. A new design, denoted Flexible Tab-Assisted Control (FlexTAC) and sponsored by the NAVSEA SUB-RT Advanced Submarine Technology Office, uses Shape Memory Alloy (SMA) wires to deflect a compliant tab. This SMA is a Ni-Ti alloy that undergoes a phase change and finite strain in response to a change in temperature. Electrically induced Joule heating in the wires causes them to contract, thereby deflecting the tab. Removal of heating accompanied by restoring forces built into the system lead to strain recovery and is the basis for the term *shape memory*. To increase the cycle time and to be able to deflect the tab in both directions, a second set of wires is used on the opposite side of the tab. Thus, one set of wires is used to *pull* the tab back to a neutral position or to deflect it in the opposite direction while the other set of wires is cooling. This operation is denoted antagonistic control. An example of the flap with a continuous camber SMA-actuated tab is shown in Fig. 10.

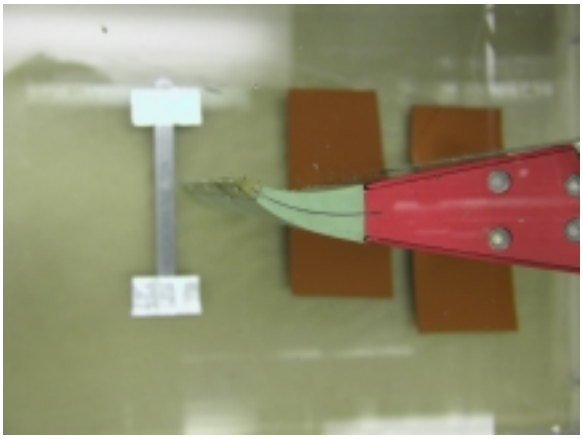

Fig 10. Flexible tab (green) on trailing edge of flap (red)

FlexTAC has been tested in a water tunnel at 1/8-scale[129], and numerical work to predict forces and moments acting on the appendage and to conduct shape optimization studies has been completed[130]. The results show that small deflections (up to 10°-12°) of the tab effect linear changes in appendage lift up to 27% and up to 43% for flap lift, and this behavior is largely independent of flap and attack angles. Furthermore, small tab deflections linearly vary flap torque and can reduce it to zero without a significant lift penalty for most test conditions. Two FlexTAC advanced sternplanes will be tested on a 1/20th-scale radio-controlled submarine model later this year, and on the Navy's 1/4-scale submarine (LSV) in two years.

Quackenbush, et al.[131-134] have tested SMA-actuated oscillating control surfaces for the purpose of introducing a secondary vortex system in order to mitigate the primary vortex wake of control planes mounted on a submarine sail. They use the term *vortex leveraging* to refer to the interaction of secondary vortices with the primary vortex system to accelerate existing natural instabilities to lead to break-up and dissipation. Hence the SMA-actuated planes are referred to as Smart Vortex Leveraging Tabs (SVLT). Submarines often operate somewhat buoyant for safety reasons; therefore, submarines equipped with sailplanes typically deflect them to a small dive angle to provide a downward force on the vehicle during cruise conditions. This operation produces a vortex pair with upwash with obvious implications for stealth. Computations and experiments using an SMA-actuated tab in a water tunnel and a mechanically-actuated tab in a tow tank have demonstrated vortex wake break-up and the overall feasibility of the concept. They plan to further test the concept on the LSV or a full-scale submarine. A simulation of the proposed system installed on a Los Angeles class submarine appears in Fig. 11.

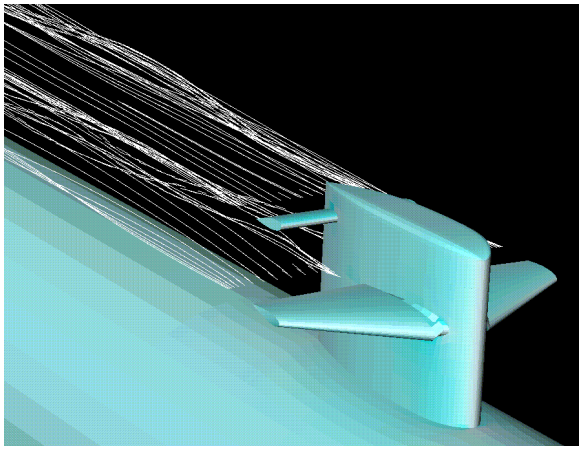

Fig. 11 Simulation of installed SVLTs on a Los Angeles class submarine.

3.13 Thrust Vectoring

Gilyard and Bolonkin[135] used simplified equations of motion to estimate the ideal, or optimal, thrust-vectoring angle for each flight phase of an aircraft. For take-off, the objective is to minimize the distance to rotation. The ideal thrust-vector angle was approximately 12 degrees, noting that the thrust-to-weight (T/W) ratio dominates this determination with increased T/W giving increased thrust-vector angles (and benefits).

Conventional thrust vectoring technology uses massive turning vanes to deflect the flow in the desired direction. Such a means involves a heavy vane system. This concept, currently under consideration for the Joint Strike Force fighter, has been successfully demonstrated in ground-based scale-model to in-flight tests on an F-18 configuration.[136] The configuration, referred to as F-18 HARV (high angle of attack research vehicle), was modified to accommodate a three vane thrust vectoring control system. The results indicate that more vanes lead to better performance than a single vane. The desired jet exhaust deflection angles were achievable; however, with an expected loss in axial thrust. The in-flight test showed pitch and yaw vectoring control of 0.9 and 0.6 degrees (respectively) of plume deflection for every degree of vane deflection.

During the past few years, steady blowing techniques have been tested and show promise for diverting the primary engine jet flow some 15 degrees from the centerline. The blowing techniques have generally relied on engine bleed to achieve the mass flows required for the control approach.

Recently, oscillatory excitation has been demonstrated at low speeds ($M<0.1$) to vector a jet flow some 8 degrees from the centerline.[137] For this experiment, piezoelectric synthetic jets were used as the driving effector; hence, no engine bleed was required. Rather, only power leads would be necessary to drive the effectors. The benefits of reduced weight and maneuverability are attractive to both military as well as commercial applications. Research should proceed with the development of novel effectors capable of operation on high jet speeds.

In addition to the SVLT and FlexTAC applications discussed previously, shape memory alloy (SMA) actuation is currently being incorporated into a thrust-vectoring concept. Specifically, circumferential SMA actuation devices have been embedded into the duct of a propulsor to create a Smart Duct[138]. The aft portion of the duct deflects to generate a side force, thereby, directing the outflow. A simulation of the concept is depicted in Fig. 12. A 1/12-scale technology demonstrator is under construction and will be tested in the NSWC 36” water tunnel in the next few months. The attractiveness of this concept for naval platforms is the ability to offer integrated steering capability with reduced reliance on hydraulics, enhanced stealth and the potential for improved maneuvering.

A joint project undertaken by the Naval Undersea Warfare Center (NUWC) along with the Applied Research Laboratory (ARL) of the Pennsylvania State University and sponsored by the Office of Naval Research (ONR) has resulted in the development and testing of an Integrated Motor Propulsor (IMP) intended as the propulsion unit for an Unmanned Underwater Vehicle (UUV). The IMP is novel because

it incorporates a rim-driven propulsor and a flexible section of the duct near the trailing edge to vector the thrust of the propulsor. The flexible portion is the pink-colored region in the solid model view of the IMP shown in Fig. 13. Recent testing at NSWC[139] showed that the IMP performed better than design predictions and produced good control authority across the entire expected operating range.

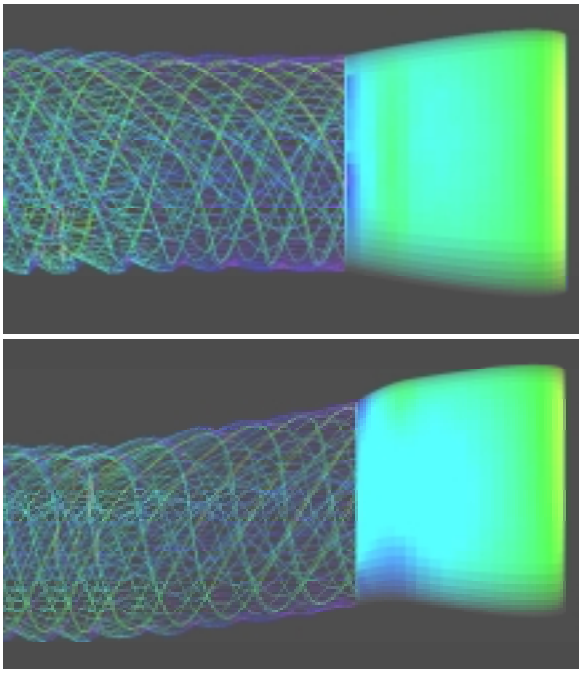

Fig. 12 Simulation of CDI Smart Duct concept.

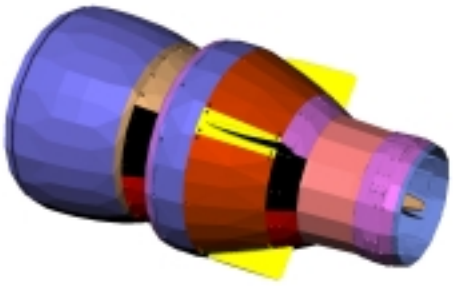

Fig. 13 Solid model rendering of NUWC/ARL UUV IMP

4. Control Methodologies

A thorough review of active flow control methodologies and their application to the control of fluid flows is an expansive topic; a proper accounting would require a separate paper. Indeed, good review papers are given by Seifert, et al.[140] and by Gad-el Hak.[141] See also a recent issue of Journal of Aircraft devoted to the subject[142] with a summary overview by McMichael.[143] An extensive list of additional references may be found in these citations.

Instead, this section will explore two diverse aspects of control. The first is active flow control with the focus restricted to two areas with potential impact on naval applications: active control of turbulent boundary layers and active control of separation from foils and bluff bodies. The second control topic will consider some current technologies and methods for automatic (or aided) control of submarine steering and depth and for fault detection. Specifically, the submarine control topic will include a discussion of the use of fuzzy logic and neural networks for advanced control system designs. Before proceeding to these two topics, we include a brief discussion of control strategies.

4.1 Control Strategies

The goal of active flow control theories is to achieve some desired objective as a function of time and space. The objectives may include drag reduction, separation control, enhanced mixing, change in a surface property, etc. In this section, open-loop, feed-forward/feedback, and optimal control theories are briefly discussed.

4.11 Open-loop control: To date, most computational (and experimental) oscillatory excitation control studies have been conducted in an open loop manner. That is, no formal, automatic control systems or philosophies were implemented. Actuation was accomplished through a variation of the actuator parameters and the resulting control was monitored, usually in an integral manner.

4.12 Feedforward/back control: The concept of feedforward (feedback) control implies that some measurable quantity in the upstream (downstream) location can serve to direct the attributes of the actuator to obtain a desired control objective downstream. For wall-bounded flows, sensing information can most readily be obtained using wall-based transducers, such as pressure or shear stress sensors. The decision whether to use feedforward or feedback control is typically dictated by consideration of the flow phenomenon under study. For studies of separation, for example, feedforward control is usually not advisable because the actuator would then be operating in the region of separation (unless the sensor is tuned to monitor the development of incipient separation) and would be less effective for control. However, if an approach were devised so that the sensors could predict the onset of separation, then a feedforward approach may be feasible. The use of feedback is usually more desirable in this case because the downstream sensors will provide the relevant information to the actuator

prior to the actuator encountering a separated flow condition. Also, the downstream sensors can measure and assess the level of control obtained due to actuation. Such feedback control was discussed by Koumoutsakos et al.[144] for turbulence control in channel flow. Examples of feedforward control as well as additional references are discussed in section 4.2.

4.13 Optimal control: Optimal control methodologies have been applied to a variety of steady or simplified flow control problems involving drag reduction, flow and temperature matching, etc. to provide more sophisticated flow control strategies in engineering applications. Optimal control theory is quite sophisticated, and its formal nature is amenable to the derivation of mathematical theorems related to existence of solutions and well-posedness of the problem. Only partial results of this type are possible in three-dimensions since, in this case, the Navier-Stokes equations themselves do not enjoy a full theoretical foundation; in two-dimensions, a complete theory is available. The reader is referred to references on optimal control theory.[145-148]

One means of obtaining this control information is to postulate a family of desired controls and an objective function (i.e., stress over a region of a foil). Through a formal minimization process, one derives a set of differential equations, and their adjoints, whose solution produces the optimal actuator profile (among the specified set). Optimal control techniques will not provide the real time control, where ultimate interest lies, but by systematically computing the best control within specified tolerances, for a given objective function, strategies (active or passive) to control a wide variety of disturbances can be developed. Optimal control can allow a determination of the best objective function to use for a given type of control and provide insight into the relationship between the time dependence of the control and the disturbances. This insight could then be built into a neural network, or other type of self-learning system, to allow effective control over a wide range of input parameters.

This methodology couples the time-dependent Navier-Stokes system with an adjoint Navier-Stokes system and optimality conditions, from which optimal states (flow fields) and controls (actuators) may be determined based on some objective functional. If control is effected through the injection or suction of fluid through a single orifice on the boundary, like oscillatory control, then the system determines whether injection or suction is warranted and at what point in time actuation is effected. As such, the approach may be useful for DNS and LES approaches, but because of the very time-dependence of the approach, it may not be useful for RANS.

Unlike feedback control methodologies where the sensed data determines the control through a specified feedback law or controller, here the time-dependence of the control is the natural result of the minimization of the objective functional. However, in the optimal control setting, the sensor is actually an objective functional and the controller is a coupled system of partial differential equations that determine the control that does the best job of minimizing the objective functional.

A self-contained methodology for active flow control[149-150] was developed using control theory and DNS. The method coupled the time-dependent Navier-Stokes system with the adjoint Navier-Stokes system along with optimality conditions from which optimal states (i.e., unsteady flow fields and controls) were determined. Although the approach is sufficiently generalized so that separation control or other problems of interest may perhaps be solved, only boundary layer transition suppression has been demonstrated with the approach. After the successful demonstration of control with optimal control theory, others have used the methodology for drag reduction in a turbulent boundary layer.[151-152]

As a final point on the use of optimal control, such capability does not come without cost. From an implementation viewpoint, the coupled system can be quite challenging to solve for three-dimensional large-time problems. The adjoint system requires that the velocity field obtained from the Navier-Stokes equations be known everywhere in the computational domain for all time. This is a substantial requirement for 2D problems. For 3D problems, the memory requirements can quickly become prohibitively expensive and involve an order of magnitude more storage. Furthermore, the computing cost can be 10 times more expensive than that for a single DNS solution. An alternate implementation might consider retaining the coefficients every 10 (or more) time-steps and still yield a quantitatively meaningful solution, thereby reducing the memory requirements by an order of magnitude. This hypothesis will require validation in a future study.

Some recent applications of optimal control for reduction of drag in the flow about cylinders,[153] for damping and control of Tollmien-Schlichting waves to delay transition,[154-155] and a presentation of second order methods for the solution of optimal control problems governed by the unsteady Navier-Stokes equations,[156] are representative examples. Finally, Choi, et al.[157] apply optimal control theory in order to develop a feedback control method for general stationary and time-dependent fluid flow problems. They test their method on the Burgers equation, which

serves as a one-dimensional model of the Navier-Stokes equations. Most of their computational cases demonstrated significant reduction in the cost. Numerous additional references may be found in these citations.

4.2 Active Flow Control Topics

This section reviews the subjects of active control of turbulent boundary layers and active control of separation around foils and bluff bodies. These fields are still young, and laboratory experiments have not yet been transitioned to field applications. An example of the latter, a submarine maneuvering application that might benefit from an active separation control system, is provided.

4.21 Active Control of TBL Evidence for potential success in the reduction of drag in fully developed turbulent boundary layers by means of active control came with the maturation of direct numerical simulations (DNS) that could reproduce the high-shear-stress-producing coherent structures that dominate the near-wall region. Actuation mechanisms that were able to disrupt these structures could then be inserted into the simulation to discover their impact on the flow. However, prior to the first DNS study, Breuer[158] developed a simpler model for these coherent structures and postulated the form that an active control scheme might take.

The model was simplified by excluding the effects of viscosity and by relying on the linear turbulence-mean shear interaction and discarding nonlinear interactions with the coherent structure. Such a simplified description is valid for short times only; however, for the purposes of control, short times are sufficient. Computations showed that the model produced shear layer structures in the vertical direction, alternating high/low speed streaky structure in the streamwise direction and strong pressure peaks. Based on these results, he postulated an active control scheme using sensors and an actuator. Four possibilities for (wall-based) sensing were suggested: 1 pressure peak detection with a pressure sensor, 2 streamwise shear stress peak detection with a shear stress sensor, differential streamwise shear stress resulting from a pair of side-by-side sensors and 4 spanwise shear stress detection using a shear stress sensor. He suggested two actuation techniques with the goal of inhibiting the intensification of the low speed streaks: 1 injection of positive or negative vertical momentum and 2 production of spanwise motions. He predicted that a distributed sensor and actuation system would be required with scales on the order of microns and response times in microseconds.

Choi, et al.[159] performed a DNS of a turbulent channel flow at Reynolds numbers (based on centerline velocity and channel half-width)of 1800 and 3300. This seminal work then applied a variety of control strategies which took the form of an input velocity at the wall proportional to (and, in most cases, in opposition to) an instantaneous velocity measured at a *detection location* just above the wall. The results were dramatic. When the control introduced a normal velocity at the wall equal and opposite to the instantaneous velocity at the detection location ($y_d^+ = 10$), a skin-friction reduction of 25% was obtained. The skin-friction reduction was determined by the change in the mean pressure gradient required to drive the flow with a fixed mass flow rate. The efficiency of the control, power saved divided by ideal power input, was computed to be 30, implying that the power input was negligible. Similarly, computations with imposition of an equal and opposite spanwise velocity at the wall produced 30% drag reduction. The application of simultaneous normal and spanwise control, equal and opposite *v and w* components, also produced a 30% reduction.

The difficulty for practical implementation of such a control scheme is clearly the requirement for knowledge of the velocity component at the detection location in the interior of the flow. Any practical scheme will likely have to rely on wall-based sensors. If one forms a Taylor series expansion for the normal velocity component at the detection location in terms of quantities evaluated at the wall, the leading term becomes $g_w = \left(\frac{\partial}{\partial z}\right)\frac{\partial w}{\partial y}\bigg|_w$. Choi, et al. showed that the correlation of g_w with *v* was strong, and a skin friction reduction of 6% was obtained with *v* control based on g_w. A similar result for *w* control based on the leading term for the spanwise velocity component was also obtained.

This experiment clearly demonstrated the potential for drag reduction with active control. Furthermore, they showed that measurable drag reduction could be achieved with wall-based sensing. Rathnasingham and Breuer[160] then built upon the earlier suggestions of Breuer, Choi, et al. and others and *experimentally demonstrated* active control of a turbulent boundary layer and accompanying reductions in u_{rms} of 31%, p_{rms} of 17% and for wall shear stress (estimated from mean velocity profiles) of 7%. The experiments were conducted in a fully developed, zero-pressure-gradient, turbulent boundary layer with $\mathrm{Re}_\theta = 1960$. They used a linear feedforward control algorithm and employed three upstream wall-based spanwise shear stress sensors, a wall-based actuator and a downstream

sensor, s_d. The point was that u' at the location of s_d could be predicted (with a maximum error of less than 3%) by the output from the three upstream sensors. The actuator was then instructed to provide an input to the flow to adjust the signal at s_d to zero. The error signal from s_d could then be used to close the loop and provide a means to adjust the actuation adaptively. The actuator was a zero net mass flow jet exiting through a streamwise-oriented slit at the wall.

Rathnasingham and Breuer[161] later extended this work by employing three actuators and three control locations in addition to the three upstream sensors. The effect of the additional actuators was to extend the range of the controlled flow beyond the actuator footprint. When the goal of the system was altered to control wall pressure fluctuations vis a vis streamwise velocity fluctuations, reductions in p_{rms} of 15-20% were reported.

Further development of a distributed system of sensors and actuators has been reported by Tsao, et al.[162]. They have successfully built an integrated system of 18 shear stress sensors and 3 magnetic flap-type actuators on a die with area 1 cm^2. Each sensor is $250\mu m \times 250\mu m$ and the actuator plates are $1mm \times 1mm$. The integration process is complex, and they report that the yield is low. Hence, no results for the integrated system have been reported. However, earlier results using a larger actuator ($4mm \times 4mm$) in a laminar flow perturbed by a vortex generator were provided. Two actuators were operated open loop at frequencies of 10-40 Hz, and hot wire sensors were used downstream of the actuators to measure the mean flow field and infer shear stress at the wall. They report a maximum 32% reduction in drag coefficient for a portion of the actuation phase when actuated at 40 Hz.

Meanwhile, progress has continued using simulations. Joslin, et al.[163] used a DNS of 2D disturbances in a flat plate boundary layer (introduced by suction and blowing through a slot) to investigate the suppression of the disturbances by wave cancellation. The latter involves the cancellation of the disturbance by the addition of a new disturbance of similar amplitude but different in phase. The study incorporated an automated system of sensors and an actuator and was operated open loop. They demonstrated a measure of wave cancellation in an open loop fashion but reported that feedback was required to optimize the amplitude and phase.

Koumoutsakos[164] reports a whopping 40% drag reduction in a DNS of a turbulent channel flow at $\mathrm{Re}_\tau = 180$ *using wall-based sensors only*. He used a 32×16 array of collocated sensors and actuators in the simulation. Here, the sensed quantity is pressure, and the control is based on local pressure gradient, which is proportional to vorticity flux at the wall. Specifically, the large drag reduction resulted from out-of-phase control of the spanwise vorticity flux. However, he makes the sobering comment that practical implementation of this control scheme would require actuators and sensors with sizes on the order of $50\mu m$ with actuator frequencies of 1 MHz.

The development of such a dense array is a daunting task, and this has led Schoppa and Hussain[165] to consider larger scale actuators providing drag reduction over an extended spatial domain. They used a DNS of turbulent channel flow at Re=1800 and 3200 (based on centerline velocity and channel half-width). In the simulation they placed a row (in the spanwise direction) of counter-rotating, streamwise-oriented vortices with wavelengths of 4 times the characteristic wall streak spacing. By zooming in on a region of *z* between a pair of vortices, the control flow has the appearance of spanwise-directed colliding wall jets. Therefore, they actually considered two control mechanisms, counter-rotating vortices and colliding wall jets, by using only one control flow but by concentrating on larger or smaller regions when computing their results. They found substantial drag reductions, 20% for vortex control and 50% for wall jet control. Interestingly, they applied the control flow in an open loop fashion. Such a control is much more desirable for practical implementation with the physical scale of the control flow being significantly larger than near wall coherent structures and with open loop actuation.

Lee, et al.[166] also considered a control flow using a reduced amount of wall information. They performed a DNS of turbulent channel flow at Re_τ=100 and 180. Actuation consisted of blowing and suction at the wall and the sensed quantity was spanwise shear stress (actually, the spanwise variation of spanwise shear stress). The new wrinkle here is the use of a neural network to learn the correlation between wall shear stresses and the required actuation to cancel normal velocities measured at $y^+ = 10$. They then used a neural network control system to reduce drag by 20%. Investigation of the weights in the trained network for various arrangements of input sensors revealed a pattern. They were able to use this pattern to deduce a simple control scheme requiring input from only 4 sensors in a spanwise row. The distance between sensors was about 20 wall units. They also estimated the efficiency to be quite high such that the required power input to produce the actuation is significantly smaller than the power saved from drag reduction.

Tardu[167] looked at local excitation of near-wall turbulence with oscillating blowing through a spanwise slot. The goal was to understand the effects of the local excitation to render the response of the turbulence more predictable and hence controllable. Then, a suboptimal control scheme with a less dense and more feasible distribution of sensors and actuators might be more practical. Results from an experiment in a turbulent boundary layer show relaminarization for a portion of the cycle as the blowing displaces vortical structures from the wall.

More recent work by Lee, et al.[168] and by Bewley, et al.[169] has resulted in the development of successful drag-reducing (16-50%) control laws from the application of optimal control theory. The drawback with this approach is that flow field information throughout the domain is required for all time. This restricts its practicality, but allows the investigators to see how optimal controls correlate with near-wall coherent structures. More practical controls can then be deduced. In fact, Lee, et al. showed that controls relying on wall pressure or spanwise shear stress work equally well as those they derived from suboptimal control theory.

Work has also concentrated on the development of new actuators that might result in the practical implementation of active flow control. Cattafesta, et al.[170] produced designs for piezoelectric flap actuators operating at frequencies from dc to their natural frequency (hundreds of Hz). They developed a model of the actuator and coupled it with an optimization method. They used this combination to design actuators with prescribed resonant frequencies while maximizing tip deflection for a given applied voltage. They then used an actuator for open loop control of separated flow from a backward-facing step. They were able to relate the flap tip displacement to the streamwise velocity fluctuations produced by the actuator. Jacobson and Reynolds[171] developed a piezoelectric flap actuator over a cavity. The point here was to modify the near wall flow by drawing fluid into the cavity and then pumping it back out in a well-defined manner. The actuator produces a pair of counter-rotating vortices that convect away from the wall. Although the vortices decay rapidly, they produce long-lasting high and low-speed streaks downstream of the actuator. The actuator was 2.5 mm wide by 46 mm long and had a resonant frequency of 330 Hz. They placed a small array of sensors and actuators in a laminar boundary layer with imposed disturbances and demonstrated transition delay and reductions of wall shear stress.

The investigations recounted here reveal that active control in a fully-developed turbulent boundary layer resulting in drag reduction is possible and results from altering or eliminating streamwise vortices near the wall. The control has evolved from the requirement of interior flow field information to quantities that may be sensed at the wall, and current research is directed toward reducing the amount of sensed information. Actuation seems to be following a two-prong approach with continuing development of arrays of sensors and actuators on the one hand and for clever larger scale and less dense actuation strategies on the other hand. The implications for naval applications are substantial. Although application to a submarine may well be some time away, smaller demonstrations on a torpedo or an unmanned underwater vehicle (UUV) may be possible in the not-too-distant future.

4.22 Active Control of Separation: This section considers some selected recent work on active control of separation processes including the unsteady loading on foils that results from dynamic pitching. A recent and extensive review for control of flow separation processes by periodic excitation may be found in Greenblatt and Wygnanski.[172] The reader is also referred to the parametric study[173] and the discussion of mechanisms[174] by Greenblatt, et al. for the problem of dynamic stall control by periodic excitation.

Faller, et al.[175-176] used a neural network controller to guide the motion of a dynamically pitching foil to produce commanded lift-to-drag ratios (L/D), and a motion which produced an optimized L/D was computed as well. The dynamic pitching of wings causes unsteady changes in lift due to energetic large-scale vorticity in the unsteady separated flowfield above the wing. They used a rectangular planform wing with a NACA 0015 cross section and a semiaspect ratio of 2.0. The wing was equipped with 15 pressure sensors spaced along the chord from the leading edge to the 90% chord location and placed at the wing root (0% span). The experiments were then repeated with the sensors moved to the 37.5% span and 80% span locations such that at the conclusion of the experiments 45 pressure time histories were available for each of the conditions tested. (In fact, for each condition, the pressure record was an ensemble average of 20 separate trials at that condition.) These conditions entailed pitching the wing from 0° to 60° at a series of pitch rates corresponding to α^+=0.01-0.20, where $\alpha^+ = \frac{c\, d\alpha/dt}{U_\infty}$ is dimensionless pitch rate, c is chord length, $\frac{d\alpha}{dt}$ is pitch rate and U_∞ is tunnel speed. This experimental data was then used to train an artificial neural network to reproduce the pressure signals for each experimental condition. The network had 47

inputs, two hidden layers of 32 nodes and the outputs were the 45 pressure time histories. The inputs consisted of angle of attack, $\alpha(t)$, and pitch rate as well as the 45 pressure predictions from the previous time step that were fed back (recursed) to become new inputs. (For the first time step, these inputs require the initial conditions for the pressure signals.) The trained network was able to successfully predict the surface pressure time histories for each of the conditions on which it was trained as well as for conditions that were purposefully excluded from training. In addition, five force and moment coefficients were determined at each of the three spanwise locations from the surface pressure data: drag coefficient, lift coefficient, normal force coefficient, tangential force coefficient and ¼-chord moment coefficient. The neural network was then expanded to have 15 additional outputs and successfully produced predictions for these quantities as well. This neural network model of wing loading as a function of motion history then became the plant model in a neural network control system shown in Fig. 14 below.

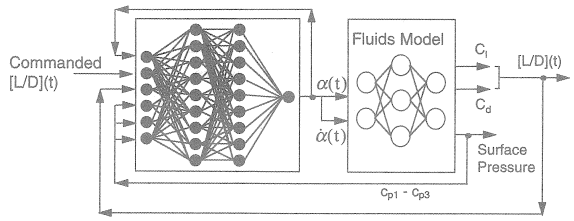

Fig. 14 Neural network controller.

To control the plant, they developed a second neural network with six inputs, two hidden layers of 12 units each and one output. The output was the angle of attack at the current time step from which the pitch rate could also be computed. (These became the plant inputs.) The controller inputs were the commanded L/D time history along with the controller output, $\alpha(t)$, from the previous time step, and plant outputs from the previous time step including L/D and three surface pressures nearest the leading edge. They used the experimental data to then train the controller on the inverse problem to predict the motion history of the wing given the L/D ratio. Their results are given in Fig. 15.

The upper graph shows the L/D response from the neural network controller for $\alpha^+ = 0.15$. The measured profile was input, the controller generated the correct motion history, and then the plant produced the predicted L/D response, which is then compared to the commanded response (measured). Note that the drag polar graph is a plot of drag coefficient vs. lift coefficient. The lower graph shows the L/D response

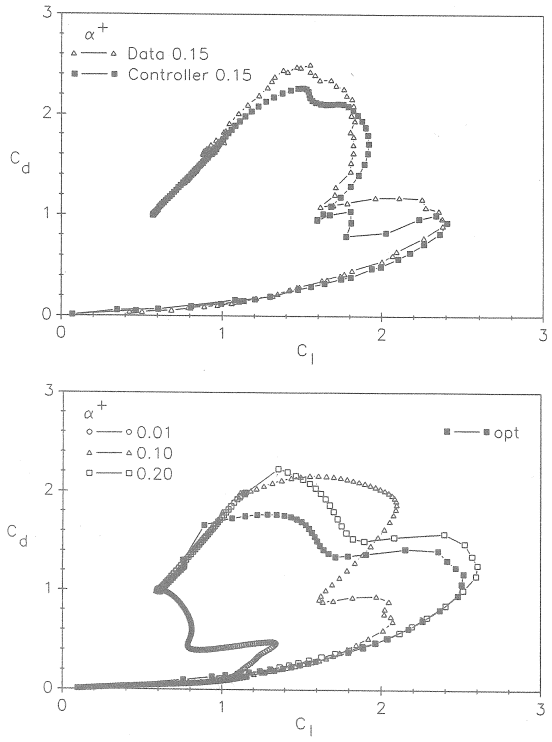

Fig. 15 Upper – Predicted and measured L/D for $\alpha^+ = 0.15$, Lower – L/D response for the optimized motion history.

for an optimized motion history; the L/D response for $\alpha^+ = 0.10$ and for $\alpha^+ = 0.20$ are shown for comparison. The reduction in drag is substantial while retaining most of the lift.

Louie, et al. [177-179] examined the effectiveness of discharging jets of water from the trailing edge of a hydrofoil to vary the circulation pattern about the foil, and therefore the lift. They then looked at the feasibility of controlling the lift variation in real time in order to cancel applied unsteady foil forces. Actuators inside the hydrofoil controlled slot openings on the pressure and suction sides of the foil. A metered supply of water from a pump provided a constant volume flow rate, and the actuators were used to divert any desired fraction of the flow to one slot or the other. The exiting fluid jetted out in a direction perpendicular to each surface. The sensor was a one-component dynamometer, which measured either lift or drag at any given time. An upstream wake generator was used to produce sinusoidal oscillating forces on the foil. A narrowband controller was used to perform the actuation in response to the force sensed by the dynamometer. Unsteady forces at the three sinusoidal harmonics were reduced by 2.0 lbs, 0.4 lbs and 0.1 lbs, respectively, as shown in Fig. 16.

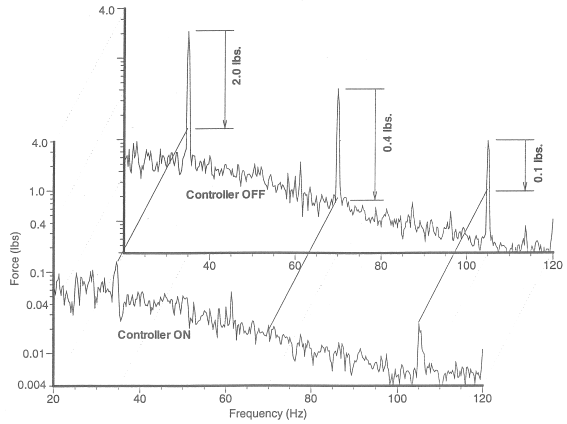

Fig. 16 Cancellation of Unsteady Hydrofoil Forces

In contrast to the previous experimental investigations, Yang, et al.[180] looked at active control of incipient unsteady separation on a pitching wing using modulated suction/injection (MSI) by means of simulation. The sensed quantity in the simulation is the spatially averaged thickness of the reverse flow, $\overline{\delta}_R$. The authors developed a control law and examined its response for combinations of Re and α^+. Their results indicate that the control law provides effective control of the unsteady separation process and leads to an increase in lift and a reduction in drag.

Seifert and Pack[181] have recently considered the impact of three-dimensionality on the separated flow over an airfoil at flight Reynolds numbers in a transonic cryogenic wind tunnel. They accomplished this by placing the foil at a sweep angle of 30° and then comparing it with the baseline flow at a sweep angle of 0°. Steady and periodic mass transfer from a slot was the control effector, and the slot location was also varied. They found that steady suction or periodic excitation was most effective and that mild sweep angle does not reduce the effectiveness of active control.

Katz, et al.[182] investigated the feasibility of delaying the separation of a turbulent boundary layer by introducing harmonic 2-D oscillations. They installed a hinged plate (75 cm long) at the end of a splitter plate in a tunnel and oriented the hinged plate at 18°. The upstream surface of the splitter plate was roughened so that a 2-D turbulent boundary layer approached the angled plate. The unforced turbulent boundary layer separated at the hinge location to form a mixing layer. Placed at the hinge location was a 10 mm long flap which spanned the tunnel. The flap was oscillated harmonically with displacement amplitudes on the order of ± 1 mm. The flap oscillation frequency was 40 Hz. When the fluctuation amplitude, u'/U as measured by a hot wire, reached 25%, the flow became completely reattached with a corresponding pressure recovery. Thus, the imposed oscillations apparently became amplified causing the boundary layer to overcome the adverse pressure gradient.

A similar type of idea was employed by Sinha[183] to delay separation around cylinders and airfoils. He developed an active flexible wall (AFW) transducer that is operated capacitively. Specifically, the substrate is composed of strips of electrical conductors with a flexible dielectric membrane stretched above the strips. The outer surface of the membrane is metallized to render it conductive. The combination acts as an array of capacitors with a shared top plate (metallized membrane) separated by an air gap. This device can act both as a sensor and an actuator. Flow-induced vibrations of the membrane are sensed as voltage fluctuations as the air gap thickness varies. For actuation an ac signal is applied to a conductive strip which then vibrates the segment of the membrane just above. The displacement amplitudes are typically of the order of $0.1\mu m$ for strip widths of 0.4-1.6 mm. These displacements are typically several orders of magnitude smaller than the boundary layer thickness. The control strategy uses the transducer elements as wall pressure sensors to detect regions of incipient separation, then the spectra are analyzed to determine the most effective actuation frequency. Selected transducer elements upstream are then actuated to reattach a separated flow or to prevent a flow from progressing to separation. Since only one or two of the transducer strips are actuated for separation control and because the displacement amplitudes are small, the actuation power is typically less than $1\mu W/m$ of span for freestream (air) velocities of 15-50 m/s. The sensing and actuation aspects of the AFW transducer were demonstrated on laminar flow (close to transition) about a circular cylinder at Re=120,000-150,000. The transducer successfully delayed separation and reduced drag by 12.4%. Particular care must be given to the thickness of the air gap and on strip width and spacing for a given application. For steady separation processes, the author expects that the device can successfully be operated open loop. Otherwise, closed-loop control with the transducer alternating between sensor and actuator modes will be required.

We conclude this short survey with interesting work by Kiya, et al.[184] in which they reduce the width of the separated region on an inclined flat plate by bombarding the leading edge of the separated region with a steady succession of vortex rings! They reason that most mechanisms currently employed for active control require actuators installed inside or on the surface of a body. They conclude that this might not always be possible and cite, as an example, (relatively

thin) blades of axial-flow compressors or blowers. Reducing separated flow around the blades is desirable, yet they are not usually thick enough to permit installation of actuators. The authors placed a 100 mm plate inclined at an attack angle of 10° in a wind tunnel at a Reynolds number of 8300. They introduced through the top wall of the tunnel through a spanwise row of five holes vortex rings generated by a woofer. Important parameters are the (shooting) frequency of generation of the rings and their circulation, both of which could be varied. The vortex rings impacted the inclined plate right at the leading edge. They were, in fact, able to reduce the thickness of the separation region with this method. When the ring impacts the plate, a strong rolling-up vortex is created on the upstream side that brings high momentum fluid in towards the surface. This influx of momentum eliminates reverse flow in the separated region on the downstream side and causes the shear layer to move in toward the surface to create a convecting *dip*. The continuing succession of vortex rings causes the leading edge vortex to continue to regenerate. A measure of success of the process is a reduction in the momentum defect in the near wake of the plate, which was experimentally measured. Finally, they estimated the efficiency of the process, defined as power saved by reducing drag divided by power required to generate the vortex rings, as a finction of shooting frequency and circulation. The maximum efficiencies were around 0.4, and they concluded that a steady round jet may not be the best choice for control in terms of efficiency.

The actuation methods reviewed here include: use of wing motion to control separation and optimize L/D, mass efflux (water jets) to counteract applied unsteady forces, steady and periodic mass transfer from slots or harmonic 2-D oscillations to delay separation, and interaction of flow structures to disrupt separation. These are but a few of many novel schemes that have shown success in the laboratory, but none have successfully made the leap to established systems in the field. Nevertheless, separation around a bluff body moving through a fluid is central to the maneuvering performance of a submarine as will be shown by the example problem in the next section. Thus, the potential impact of active separation control methods is substantial.

4.23 Submarine Maneuvering Problem: This section details a selected submarine maneuvering issue as an example which may be amenable to future implementation of active separation control technologies. Recall that in the section on Vortex and Separation Control (Section 3.8) we discussed the work of Lin, et al.[85] using micro-vortex generators (MVGs) placed on the crown of a radio-controlled model submarine (RCM). The intention was to alter the crossflow about the vehicle and to reduce the tendency of the vehicle to dive in a hard turn. The experiment was successful. The MVGs significantly reduced the dive tendency and resulted in a 20% reduction in turning diameter for the vehicle for equivalent depth excursion. Furthermore, the time required to complete the turn was reduced by 13%. Reductions in pitch and roll were recorded as well.

At the time it was theorized that shed vorticity from upstream appendages (particularly the sail) interacts with cross flow about the hull when a submarine makes a hard turn. The net effect of this complex interaction is undesirable pitch and depth changes (rise or dive) that accompany the turn. Recent experimental work by Fu, et al.[185-186] using particle image velocimetry was conducted to examine this interaction more closely and explain the process.

The experiment was carried out on the NSWC Rotating Arm. This facility is a towing carriage, which revolves in a circle and tows a *captive* submarine model (as opposed to the use of a free-running model) in a large basin of water. The model was oriented such that it was pitched at 2.0 deg (bow up), rolled 2.1 deg (to starboard) and yawed 9.5 deg to starboard. The rudder was maintained at a fixed angle of –20 deg (for a starboard turn), and the sternplanes were set to –1.0 deg (rise). These configuration values were chosen as a result of conducting steady turning maneuvers with a free-running, radio-controlled model, and these values are representative of average conditions 32 sec after execution of the maneuvers during the steady portion of the turn. A submersible PIV system was placed on the bottom of the basin in a fixed position, and the submarine model was towed through the laser sheet. A diagram of the experimental setup is given in Fig. 17.

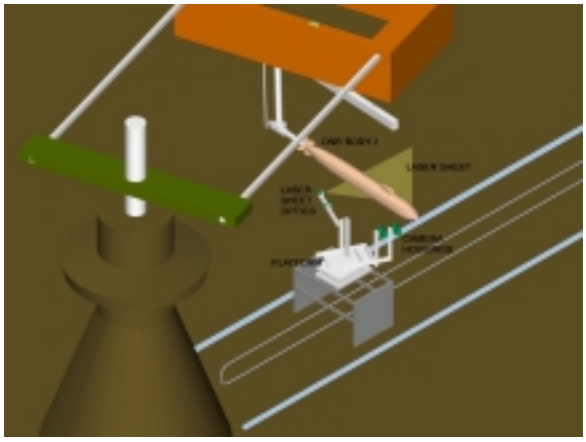

Fig. 17 Experimental setup

A series of PIV *snapshots* of the cross flow velocity field were acquired during the passage of the vehicle through the laser sheet. Note that the measurement

planes, as represented in Fig. 18, are oriented in a changing fashion at successive stations along the model, due to the fact that the model, which is pitched, rolled and yawed, passes through a static laser sheet along a circular arc.

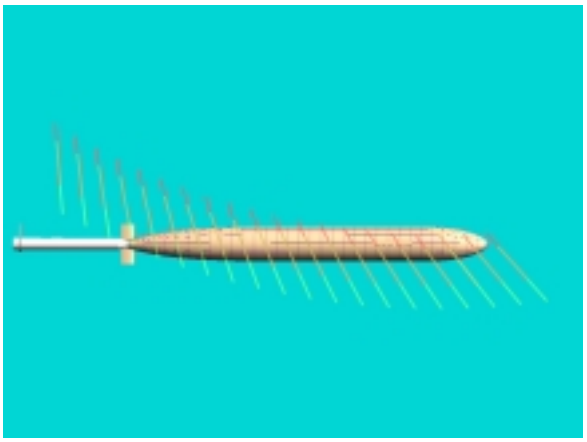

Fig. 18 Data plane locations

Two vehicle configurations were examined during these tests: the baseline configuration without MVGs, and the successful arrangement of six MVGs on the deck of the submarine that was used earlier by Lin, et al.[85] Typical PIV images obtained during the experiment are provided in Fig. 19 and Fig. 20.

Figure 19 shows an example of the velocity (represented by vectors) and vorticity fields (represented by contours) in a cross plane in the upper inside quadrant, downstream of the sail, looking aft for the configuration 1 without MVGs. The plane of measurement is the tenth plane from the nose of the model as shown in Fig. 18. The thick-lined curve represents the location on the submarine body where the laser sheet hits the model. The area between the thick-lined curve and the thin-lined curve (in gray) represents the area contaminated by the bright diffuse reflection off the body, rendering data in that region unreliable. Evident in the measured flow field and vorticity contours is a prominent trailing vortex around y = 1.2 ft. and z = -1.1 ft., which originated from the tip of the sail of the model undergoing a steady turn. At the instance of measurement, the model heading is approximately out of the page, with the sail mounted on top. Because the model is undergoing a mildly severe turn and is pitched up slightly and yawed to starboard, the local angle of drift and cross flow velocity geometrically dictates that a region of flow separation is expected on the leeward side of the body, slightly towards the deck. The velocity and vorticity field in Fig. 19 show a region of negative vorticity around y = 1.1 ft. and z = -0.2 ft., being shed in the starboard area, and a region of positive vorticity (CCW, partially out of view) on the deck of the model (z = -0.8 ft). These two regions represent points of flow separation commonly observed around a bluff body in a cross flow; however, they appear to be rotated clockwise from what is normally expected, judging from the direction of local angle of drift and cross flow velocity alone. The region between the two separation points is normally a region of low vorticity, as observed in Fig. 19.

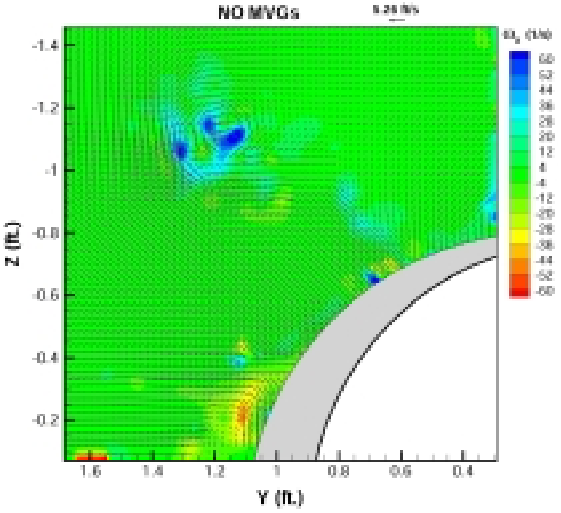

Fig. 19 Cross flow velocity and vorticity field, no MVGs

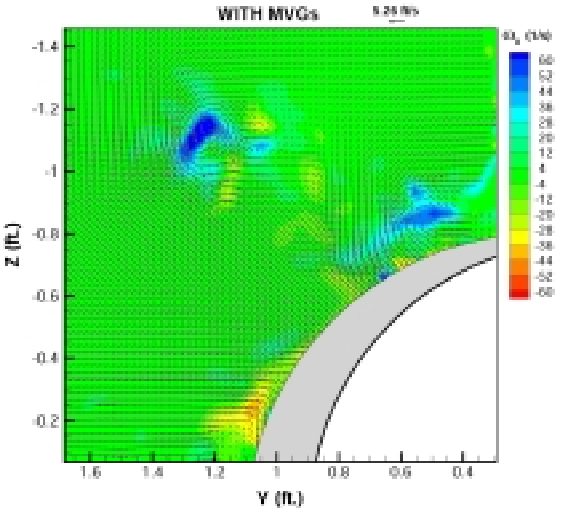

Fig. 20 Cross flow velocity and vorticity field, with MVGs

The conclusion drawn was that the sail tip vortex, due to its strength and proximity to the body, will tend to delay the starboard separation and enhance the deck separation. This is accomplished by effectively imposing a negative circulation (CW) around the body such that the separation points will rotate clockwise, as observed in Fig. 19. Because the separation zone is an area of low pressure (with a corresponding area of high pressure on the opposite side of the hull), the

aforementioned mechanism which causes the low pressure region to rotate towards the deck, contributes to an upward force on the hull aft of the sail. Since the trailing vortex originates around the tip of the sail and the CG on the model is situated close to the trailing edge of the sail, the interaction of the sail tip vortex with the hull exerts most of its influence aft of the CG. An upward force, which acts primarily aft of the CG, will result in a net downward pitching moment, consistent with the previously measured results.

Fig. 20 shows a comparable flow field, but in this case the submarine model is fitted with MVGs. Evident in Fig. 20 is the existence of a prominent large-scale vortical structure with counter-clockwise (positive) circulation around the deck of the model. This region of high vorticity is likely the result of tip vortices shed from the MVGs themselves. The tip vortices from each MVG section are like-signed and would tend to roll-up into a larger single vortical structure. Because this vortex is very near the body, it serves to bring high momentum fluid into this region of otherwise low pressure and will effectively reattach the boundary layer, working much like MVGs on an aircraft wing. This delay of flow separation on the deck in the aft section will in effect result in a pressure recovery, netting the model a downward vertical force aft of the sail and a corresponding positive pitch-up moment.

Computations based on solving the incompressible Reynolds-averaged Navier-Stokes (RANS) equations were conducted by Sung, et al.[187] for the prediction of the cross flow around a steady turning submarine. The predicted crossflow and vortex interaction compared well with the experimental results.

This submarine maneuvering example illustrates how interaction of shed vorticity interacts with asymmetric separation from the hull to produce lift on the vehicle resulting in pitching moments. However, the steady experiment cannot explain the conditions that prevail on a free-running model immediately after execution of the turn during the unsteady phase of the maneuver. Nevertheless, the passive MVGs worked well. However, an active separation control system, which could be turned on and off at will, and which could be tailored to specific maneuvering conditions would seem to be an ideal solution for this problem. Any such system would have to be able to operate under the rigorous conditions described earlier and not violate stealth requirements.

4.3 Advanced Control & Monitoring of Submarines

A submarine is a rigid body that moves through a fluid with six degrees of freedom: three which describe linear motions such as velocity components, and three which describe angular motions such as angular velocity components (roll, pitch and yaw rates). Automatic control systems have been devised to control all of these state variables; however, the primary systems are: course (steering) control, pitch and depth control, roll control and speed control. Early versions of these systems began with the development of modern control theory techniques beginning in the 1950's. However, to design controllers for the needed multi-input/multi-output systems (MIMO) required more sophisticated design techniques based on the linear quadratic Gaussian (LQG) stochastic control problem with loop transfer recovery (LTR) for increased robustness. Much of the research applying LQG/LTR multivariable control design methodology to automatic depth and course control of submarines was conducted at MIT in the mid-1980s. Gibson, et al,[188] give an accounting of this work and describe the increasing sophistication of submarine control systems.

Beyond the need for such control systems (whether aided or automatic) to support the crew in operating the ship, are advanced control functions such as *control reconfiguration* in the context of recovery. Here, we refer to the need to switch to an alternative control system to be employed in the event that the plant changes as a result of damage or modifications in the environment. To determine if such a change is necessary a monitoring function must be utilized to: *detect* a fault, *identify* the fault, *diagnose* the fault and initiate *recovery* actions to remove the effect of the fault (such as control reconfiguration). Together, these requirements form the basis of an Advanced Control and Monitoring (ACM) system. Ammeen and Faller[189] and Ammeen and Beale[190] give detailed descriptions of such a system and a discussion of the current research proceeding to implement it. Some of the fault diagnosis and performance monitoring capabilities exist on current submarines such as *Seawolf*. Hammett, et al.[191] provide a description of the latter system.

New technologies are being employed for control system and ACM development including fuzzy logic and neural networks. A selection of some of the research in these areas for submarine applications follows.

4.31 Fuzzy Logic: This discipline refers to the mathematical framework that has been devised to express subjective information (human imprecision or vagueness). An alternative view is that the mathematical foundation gives the user a diverse and rich set of tools to describe real-world problems of many colors vis a vis simplistic black-and-white issues. An excellent first tutorial on the subject is given by Mendel.[192-193]

Modeling requires that functional relationships be established, such as $y = f(x)$ for example. This is a

mapping of a *crisp* input, *x*, into a crisp output, *y*. Here crisp is used to mean a definite, precise value as opposed to a fuzzy value. Fuzzy logic can be used to map crisp inputs into crisp outputs, but internal to the model, fuzzy concepts based on a set of rules are employed to implement the mapping. This requires that a system, called a fuzzy logic system (FLS) be used, and it often takes the form shown in Fig. 21.

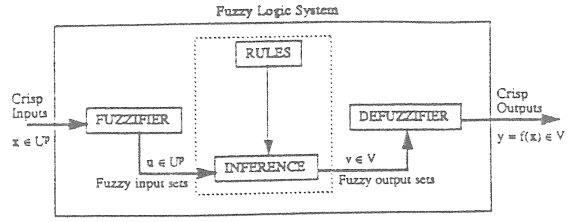

Fig. 21 Fuzzy logic system, taken from Mendel.[192]

A *fuzzifier* takes crisp inputs and places them into fuzzy sets. The rules take the form of IF-THEN statements. The *inference engine* decides which rules to employ and then maps members of the input fuzzy sets into output fuzzy sets. Finally, the *defuzzifier* converts fuzzy values back into crisp values for output.

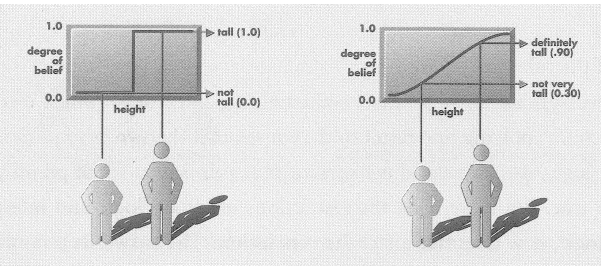

Fig. 22 Membership functions for a fuzzy set taken from Matlab reference.[194]

To make this a bit clearer, we need to explain how values are placed into fuzzy sets. The following example comes from a Matlab reference.[194] Consider the set of tall people, and allow the input space to range from 3 ft to 9 ft. To place people as members of a crisp set, one might impose a condition such as, "all people greater than 6 ft are officially considered tall". The membership function shown on the left in Fig. 22 formalizes this statement, and demonstrates the sharp boundary of a crisp set. However, experience dictates that calling one person short and another tall, when their height may vary by only an inch, is unreasonable. Furthermore, the definition of tall people may change depending upon context. How does the tall person definition change when considered by a basketball player? Instead, saying that tall person membership is a *matter of degree* might render the definition more workable. Thus, the tall-person definition might be described by the membership function, denoted $\mu(x)$, shown on the right in Fig. 22. Using such a definition, one can say that two people may be tall, but that one is definitely taller than the other is. A membership function is mathematical formalism for the vague (*fuzzy*) linguistic terms just described, and the set of tall people characterized by that membership function is a *fuzzy set*.

An interesting fact about fuzzy sets is that a member may simultaneously reside in more than one fuzzy set to different degrees. Mendel[192] considers the set of foreign cars and domestic cars with membership functions $\mu_F(x)$ and $\mu_D(x)$. Suppose that the variable *x* represents the percentage of parts manufactured domestically. A given car with 75% of its parts made locally might have $\mu_D(75\%) = 0.9$ and $\mu_F(75\%) = 0.25$. For a fluid mechanics application, one might consider the set of fluid elements residing in a boundary layer, and the set of fluid elements in the free stream. Precisely where is the edge of the boundary layer? Is there a crisp definition? One might base the membership functions on the percentage of free stream speed that the local velocity has reached, such that members may reside in both sets to differing degrees: $\mu_{BL}(90\%) = 0.7$ and $\mu_{FS}(90\%) = 0.4$. One might then build a set of rules. If an element is deep within the boundary layer, in the sublayer, then viscous effects are very important, perform action 1 vigorously. If an element is in the log region, then viscous effects and inertial effects are of the same magnitude, perform action 2 moderately. If an element is in the free stream, then viscous effects are unimportant, perform action 3 mildly. The shapes of the membership function curves can rigorously handle these fuzzy definitions; the curves are prescribed by *experts* or by extracting the knowledge from experimental data. The set of actions that are executed in response to the input fuzzy sets are themselves members of a fuzzy set with corresponding membership functions. The response or action taken is defuzzified, and an output is given. This may be a numerical value, which is sent to a transducer, say.

There exists a tremendous amount of information on fuzzy logic in the literature. A few additional references on fuzzy logic systems are: Takagi and Sugeno[195] with industrial applications, Mendel and Mouzouris[196] for the predictive modeling of nonlinear systems, Mendel[197] for signal processing applications, and Johnston[198] for applications to control.

Fuzzy logic systems have found application to submarine depth control systems. Near the free surface submarine depth-keeping can be complicated by such effects as low speeds, seaway condition, surface suction and buoyancy effects. Away from the free surface, the

vehicle should proceed from one depth to another depth rapidly and with minimal error. In addition, the controller needs to be robust with regard to plant modeling error. These issues were recognized by Choi, et al.,[199] and through simulation and experiment, they implemented a fuzzy logic system for depth control. The system is based on heuristic control rules of an expert operator, which are listed below.

1. *When preparing for a large depth change, the operator deflects the dive planes to get the desired pitch angle.*
2. *If the desired pitch angle is achieved, the operator returns the dive planes to an undeflected position.*
3. *The operator maintains the desired pitch angle until the vehicle nears the desired depth.*
4. *As the vehicle approaches the desired depth, the operator deflects the planes to get a zero pitch angle.*
5. *To reach the final desired depth, the operator manipulates the planes as required to minimize the depth error.*
6. *When maneuvering to maintain depth, the operator heuristically determines an appropriate dive plane angle. The latter is dependent upon attack angle and vehicle buoyancy and trim conditions.*

For the simulation they employed the submarine equations of motion for heave (vertical motion) and pitch, and made the controller adaptable to variations in vehicle speed and departures from neutral buoyancy. They also incorporated some safety logic, which amounted to basic fault detection procedures. They investigated three specific scenarios in the simulations: depth changing with varying speed, depth keeping with varying speed and depth keeping with varying buoyancy. They report that the simulations successfully demonstrated the ability of the fuzzy logic controller (FLC) to handle all three scenarios. Sea trials of a submersible vehicle were then conducted, and the behavior of the vehicle using the fuzzy logic controller was compared to that using an existing linear quadratic (LQ) controller based on a linearized model. The experiments showed a reduction in control plane activities and greater insensitivity to modeling error and uncertainties when using the FLC. They report significant difficulty in choosing appropriate scaling factors and suitable membership functions when implementing the FLC for the submersible vehicle and are looking into alternative schemes for defining these quantities.

Ammeen and Beale[200-201] also looked at application of fuzzy logic to depth control. They designed a fuzzy depth control algorithm, and then demonstrated that the fuzzy controller was equivalent to a gain-scheduled proportional plus derivative (P-D) controller. This was a convenient finding as the existing time-varying gain controller had already been subjected to a rigorous stability analysis. They then employed Kharitonov theory and Lyapunov theory to demonstrate stability of the closed-loop system (submersible model and fuzzy depth controller) over all allowed values of the controller. Such a rigorous determination of stability robustness is critical for tactical use of submarine controllers.

Proceeding beyond depth control, Kim, et al.[202] combined a neural network fault detector and a fuzzy logic decision module into a Failure Detection System which could then be incorporated into a general fault tolerant control system. They demonstrated the system for detection of failures (lock-ups) in the two control surfaces on a single-waterplane-area twin-hull (SWATH) surface vehicle. Specifically, the neural network had 16 inputs, two hidden layers with 16 nodes each and one output. The inputs included the pitch and depth of the vehicle along with four past values for each, and the current and two previous values for the two control surfaces on the vehicle. Based on this input information, the network was trained to produce an output value that converged to 0.5 for normal operations, to 0.2 for controller lock-ups at negative angles and to 0.8 for controller lock-ups at positive angles. The neural network output was then sent to the fuzzy decision algorithm, where it was then placed in one or more of the fuzzy input sets depending upon the membership functions for each. The three fuzzy input sets were defined: small (S), medium (M) and large (L). Two fuzzy output sets, control (C) and failure (F), were also defined with appropriate membership functions. Thus, the crisp output from the neural network, *xout*, gets fuzzified and placed in S, M or L. The following rules are applied to map the fuzzy inputs sets S, M and L into the fuzzy output sets C and F.

1. *If xout is S, then fout is F.*
2. *If xout is M, then fout is C.*
3. *If xout is L, then fout is F.*

Then, a defuzzification process is applied to map the fuzzy output sets to a crisp value smoothly varying between 0 and 1, where 0 = no failure and 1 = failure. This is the essence of a fuzzy logic system defined earlier. They applied the system to detect failures on the SWATH configuration. Their system correctly detected simulated failures with no false alarms and demonstrated the feasibility of such a system. They noted that insertion of such a system into real applications would require the ability to detect multiple failures in a more realistic environment containing sensor noise and nonlinear and time-varying dynamics.

This last reference illustrated the utility of a fuzzy logic system as well as the potential for neural networks. The next section will explore the use of neural networks for naval applications in greater detail and show how they may be employed for fault detection and control reconfiguration.

4.32 Neural Networks: A neural network is a computational technique for developing time-dependent nonlinear equation systems that relate input variables to output variables. A *recursive* neural network (RNN) is one that employs feedback; namely, the information stream issuing from the outputs is redirected to form additional inputs to the network. An RNN is typically employed when time-dependent predictions are necessary and some memory of the process is required. The Neural Network Development Laboratory at NSWC was established in 1994 with the directive to apply neural network technology as a predictive tool for naval applications. That effort has, since then, been successful in a wide variety of applications; however, a significant portion of the work has been directed towards the prediction of the time histories of maneuvering variables of a submarine executing submerged maneuvers. This latter simulation is currently being employed as a plant model for the development of an advanced control and monitoring system (ACM). Therefore, some attention will be given to the history of the neural network efforts at NSWC followed by a detailed description of the submarine plant model. Then, some current research toward the development of the ACM will be described, followed by a few examples of ongoing efforts elsewhere.

NSWC recognized that neural networks might become a useful submarine maneuvering simulation tool as a result of work using RNNs to predict and control three-dimensional unsteady separated flow fields[175] and dynamic reattachment.[203] The subsequent development of an RNN-based simulation tool for submarine maneuvering was documented by Faller.[204-205] RNN simulations have been created using experimental training data derived from both model and full-scale submarine maneuvers. In the latter case, incomplete data measured on the full-scale vehicle was augmented by using feedforward neural networks as *virtual sensors* to intelligently estimate the missing data.[206] The creation of simulations at both scales permitted the exploration of scaling differences between the two vehicles.[207] Neural network simulation techniques have also been extended to the development of simulations of surface ship maneuvers. Hess[208] describes an initial formulation of the problem using an RNN model for use with ships. The method was then further refined and produced accurate predictions of tactical circle and horizontal overshoot maneuvers.[209] The topic of Real-Time Nonlinear Simulation (RNS) and control of maneuvering vehicles is introduced and described by Faller.[210] Recently, the neural network maneuvering simulation tool was used to make blind predictions of submarine maneuvers,[211] and these predictions were then compared with results using other techniques. Finally, Ammeen and Faller[189] and Ammeen and Beale[190] describe the development of an Advanced Control and Monitoring system incorporating the RNN simulation as the plant model.

An RNN with the ability to predict the time histories of maneuvering variables of a submarine executing submerged maneuvers can then be used as a plant model within an advanced control system. A description of this RNN follows. The input data required by the RNN consist only of the initial conditions of the vehicle and time histories of the control variables: propeller rotation speed and rudder & sternplane deflection angles. As the simulation proceeds, these inputs are combined with past predicted values of the state variables (outputs) to estimate the forces that are acting on the vehicle. The resulting outputs are predictions of the time histories of the six-degree-of-freedom state variables: linear and angular velocity components which can then be used to recover the remaining hydrodynamic variables required to describe the motion of the vehicle. A schematic representation of the technique is shown in Fig. 23.

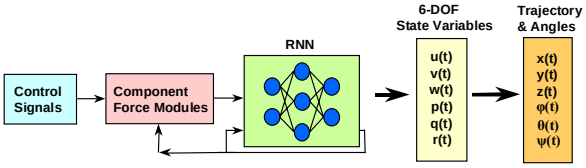

Fig. 23 RNN submarine simulation.

The architecture of the neural network is illustrated schematically in Fig. 24. The network consists of four layers (groupings of nodes): an input layer, two *hidden* layers and an output layer. Within each layer are nodes, which contain a nonlinear transfer function that operates on the inputs to the node and produces a smoothly varying output. The binary sigmoid function is used; for input x ranging from $-\infty$ to ∞, it produces the output y that varies from 0 to 1 and is defined by $y(x) = \frac{1}{1+e^{-x}}$. The nodes in each layer are fully connected to those in the next layer by weighted links. As data travels along a link to a node in the next layer it is multiplied by the weight associated with that link. The weighted data on all links terminating at a given node is then summed and forms the input to the transfer function within that node. The output of the transfer function then travels along multiple links to all the nodes in the next layer, and so on. So, as shown in Fig. 24, an input vector at a given time step travels from left to right through the network where it is operated on many times before it finally produces an output vector on the output side of the network.

A recursive neural network has feedback; the output vector is used as additional inputs to the network at the

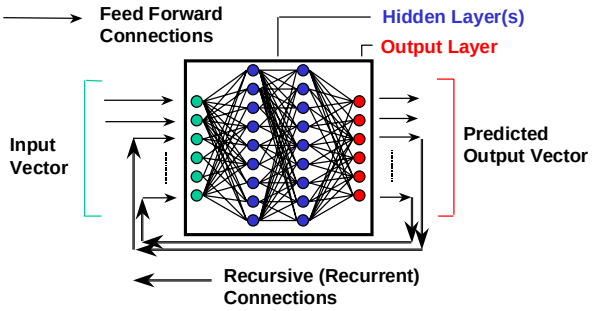

Fig. 24 Recursive neural network architecture.

next time step. For the first time step, when no outputs are available, these inputs are filled with initial conditions. The time step at each iteration represents a step in dimensionless time, $\Delta t'$. Time is rendered dimensionless using the vehicle's length and its speed computed from the preceding iteration; thus, the dimensionless time step represents a fraction of the time required for the flow to travel the length of the hull. The neural network is stepped at a constant rate in dimensionless time through each maneuver. Thus, an input vector at the dimensionless time, t', produces the output vector at $t' + \Delta t'$.

The process by which the network is iteratively presented with an input vector in order to produce predicted outputs that are then compared with a desired output vector is known as training. The purpose of training is to gradually modify the weights between the nodes in order to reduce the error on subsequent iterations. In other words, the neural network *learns* how to reproduce the correct answers. When the error has been minimized, training is halted, and the resultant collection of weights that have been established among the many connections in the network represent the knowledge stored in the trained neural net. Therefore, a training algorithm is required to determine the errors between the predicted outputs and the desired target values and to act on this information to modify the weights until the error is reduced to a minimum. The most commonly used training algorithm, and the one employed here, is called backpropagation which is a gradient descent algorithm. The collection of input and corresponding target output vectors comprise a training set, and these data are required to prepare the network for further use. Data files containing time histories of control and state variables for a submerged maneuvering submarine are used to effect the training.

After the neural network has been successfully trained, the weights are no longer modified and remain fixed. At this point the network may be presented with an input vector similar to the input vectors in the training set (that is, drawn from the same parameter space), and it will then produce a predicted output vector. This ability to generalize, that is, to produce reasonable outputs for inputs not encountered in training is what allows neural networks to be used as simulation tools. To test the ability of the network to generalize, a subset of the available data files must be set aside and not used for training. These validation data files then demonstrate the predictive capabilities of the network.

As an example of the fidelity of the simulation, Hess[211] cites the following results during a recent Submarine Maneuvering Simulation Challenge in which the RNN submarine simulation was used to predict blind maneuvers. The RNN simulation was used to produce predictions for 78 known runs (that is, the answers were also provided) and 34 *blind* maneuvers of a radio-controlled submarine. An independent arbitrator graded the 34 *blind* runs and assigned 32 grades of Good and 2 grades of Fair, and this was the highest total score obtained by any participant for the blind predictions. The simulation required 3 man-weeks to develop the 112 maneuver predictions, and no additional time was spent in an effort to optimize the results. The solutions were developed on PC-based platforms requiring approximately 200 CPU hours to train offline; however, the trained neural network produced the predictions faster than real time requiring a fraction of a second per prediction.

Ammeen and Faller[189] describe the integration of tactical submarine control algorithms with the RNN submarine plant model described above for the purpose of submarine fault detection & isolation and control reconfiguration. The idea is shown in Fig. 25.

The controllers shown in Fig. 25 are the tactical automatic steering and diving algorithm. The fault detection module compares the appropriate platform parameters with the output of the RNN. This block determines when a fault has occurred. The decision module classifies the fault; that is, it attempts to diagnose the fault or determine what has failed. This information is sent to control switching logic, which, based on the particular fault, reconfigures the control system appropriately to maintain stability and control. Thus, the switching logic turns to controller B or controller C, etc. Other recovery approaches can also be applied, such as flying through the condition under automatic control and providing the operators with specific recovery information (via operator aids). The system has been demonstrated to provide rapid detection and accurate classification of faults. The implementation of the reconfigurable control aspect is currently under development.

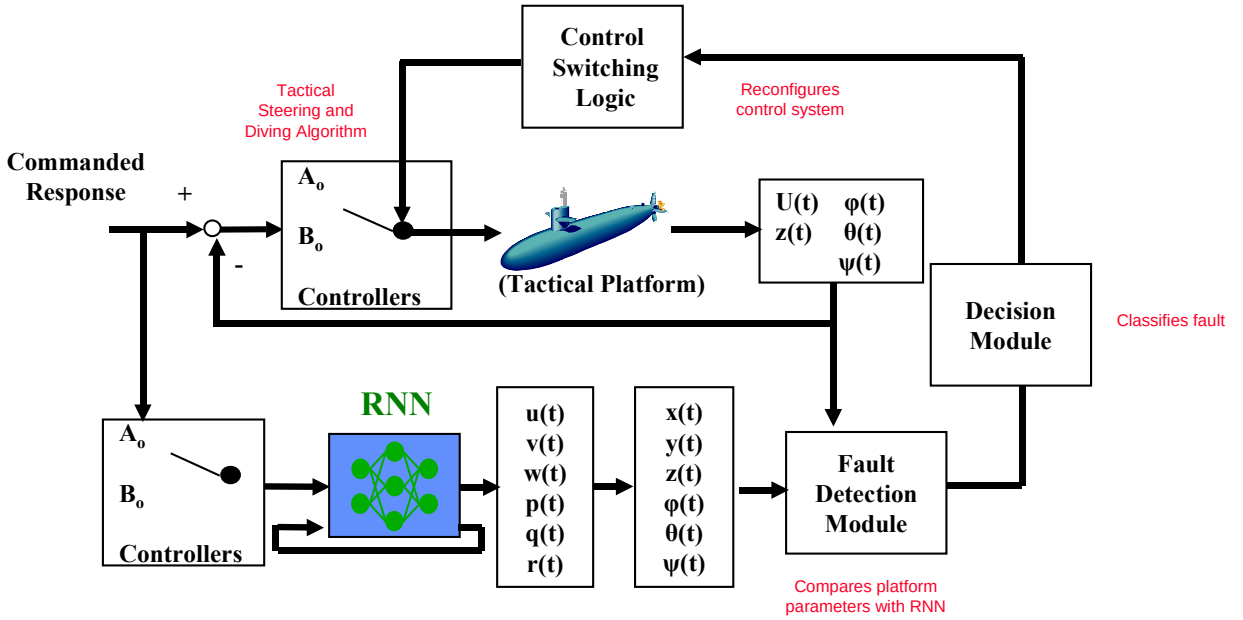

Fig. 25 RNN-based Submarine Advanced Control and Monitoring System

Elsewhere, neural networks are in use or are planned in several applications. They have been used to assist a time-domain numerical model for prediction of pitch and heave motions of a trimaran frigate in regular head seas.[212-213] Experiments conducted to complement the calculations were then used to train a neural network to predict pitch and heave motions for wave frequencies not contained within the training data. Also in the domain of ship research is the station-keeping (dynamic positioning) problem that has been considered by Li and Gu.[214] They devised a neural net controller to maintain horizontal position in the presence of wind and wave motions, and then tested it under simulated conditions within a computer. Burns and Polkinghorne[215], Logan[216] and Witt and Miller[217] discuss neural network-based autopilots for optimal guidance of surface ships.

Sutton, et al.[218] present the results of a simulation study into the development of a neural network controller for depth control of a UUV. The compared the results of the NN controller with a PID controller and found that the NN controller performed better. Norton[219] describes kinematic motion control of simulated autonomous underwater vehicles. He used a neural network, which accepted range, bearing and heading information to produce a speed and rudder angle. Venugopal, et al.[220] discuss the use of multilayer neural networks as adaptive controllers for autonomous underwater vehicles (AUV). In particular, two adaptive control schemes, for direct and indirect control, are examined. Finally Mort, et al.[221] use a neural network controller for control of multivariable models. They demonstrate their technique on analytical models of a surface-piercing hydrofoil and a deeply submerged submarine. They also offer an early look at reconfigurable control techniques in the event of an actuator failure.

5. Concluding Remarks

This survey of passive and active flow control technologies was conducted to showcase the challenges and potential, and the successes and failures of the devices and systems for use on Naval platforms, particularly submarines. In hindsight, the scope was probably too large. The task has proved most challenging because of the diversity in the experiments, measurements, results, and conclusions published and vast number of publications in each flow control technology. Many of the technologies, although technically feasible, have not been incorporated in a production application for economical, operational, infrastructural, or other non-technical reasons.[222] Where we had to make decisions regarding the inclusion of papers, we tended to incorporate the most recent works and tried to direct the interested reader to further review papers.

Much of the literature regards *active* flow control as a control scheme employing open-loop actuation as opposed to the use of a passive device. Thus, active flow control does not necessarily imply closed-loop flow control with actuators directed by sensor feedback, although it can mean exactly that. The number of closed-loop active control applications is still relatively small and largely confined to the laboratory.

Submarines can clearly benefit from the use of micro-vortex generators, circulation control using coanda wall jets, advanced control surfaces actuated by smart materials and advanced thrust-vectoring techniques. The use of polymers for drag reduction faces severe storage and handling uses. Lorentz force pumping for drag reduction seems to work, but the efficiency has not yet been proven to be high enough to make the technique practical. Nevertheless, the actuation is *quiet*, and this drives the search for possible alternative uses. The use of microbubbles also faces efficiency questions and is largely restricted to near-surface use. Active closed-loop control of turbulent boundary layers and separation are exciting fields and show much promise. These technologies are likely to find future application on Naval platforms. The use of fuzzy logic systems and neural networks as components of advanced control and monitoring systems for submarines is well advanced. Elements of this technology already exist on some submarines.

Other technologies discussed in this paper may achieve successful incorporation into civilian or military production configurations either after adequate design tools are available for the flow control technology or after larger-scale testing yields higher technology readiness of the technology. Finally, some of the flow control technologies may reach sufficient technology readiness for a military configuration that the initiative may potentially become classified.

Drawn out by this study, it has become clear that as the technology becomes more sophisticated (passive versus active), the benefits must be sufficiently high to warrant the additional risk of a more complex system, whereas risk is not necessarily technical but rather financial. New complex systems lead to uncertainty in estimating manufacturing, operational, and overall life cycle cost for the new configuration. If uncertainty is too high versus the benefit margin, then the technology will not reach a production application.

Acknowledgements

The authors would like to thank Ronald D. Joslin of the Office of Naval Research for his significant contributions to sections 2, 3 and 4 and for his many helpful comments and suggestions for this paper. His contributions are used with permission. We are also grateful to Jerome P. Feldman, Robert F. Roddy, Jr., Edward S. Ammeen, James D. Gibson, Stuart D. Jessup, and Ernest O. Rogers of NSWC for their input and suggestions. Input from Christopher J. Egan, Office of Naval Research, and Daniel P. Thivierge, Naval Undersea Warfare Center, is also greatly appreciated. We also wish to acknowledge the support of the Office of Naval Research, Codes 333, 342 & 351, (L. Patrick Purtell, Ronald D. Joslin and Promode Bandyopadhyay) and the NAVSEA Advanced Submarine Technology Office, SUB-RT3, (Douglas J. Dahmer and Steven Weinstein) for the support of work performed at NSWC.

References

1. Joslin, R. D., Kunz, R. K., and Stinebring, D. R., Flow control technology readiness: aerodynamic versus hydrodynamic. AIAA Paper 2000-4412, Aug. 2000.
2. Thomas, R. H., Choudhari, M. M., and Joslin, R. D., Flow and Noise Control: Review and Assessment of Future Directions. NASA TM-2002-211631, April 2002.
3. Gad-el-Hak M., Flow Control: Passive, active, and reactive flow management, Cambridge University Press, Cambridge, 2000.
4. Gad-el-Hak, M., Pollard, A., Bonnet, J.-P. (eds), Flow Control: Fundamentals and Practices, Springer-Verlag: Berlin, Heidelberg, 1998.
5. Lachman GV., (ed), Boundary layer and flow control. Vol. 1 and 2, Pergamon Press. 1961.
6. Burcher, R., Rydill, L., Concepts in Submarine Design, Cambridge Ocean Technology Series 2, Cambridge University Press, 1994.
7. US Department of the Navy-Naval Historical Center. http:/www.history.navy.mil.
8. Chief of Naval Operations, Submarine Warfare Division, http://www.chinfo.navy.mil/navpalib/cno/n87/history/subhistory.html.
9. Augustine, N. R., Augustine's Laws, AIAA, New York, NY, 1983.
10. Schumacher, M., Seawater Corrosion Handbook, Noyes Data Corporation, 1979.
11. Huang, T. and Feldman, J., "Methods of Predicting the Motion of Submarines," ASME Winter Annual Meeting, 88-WA/DSC-22, Nov-Dec 1988.
12. Feldman, J., "Method of Performing Captive-Model Experiments to Predict the Stability and Control Characteristics of Submarines," NSWC Research & Development Report, CRDKNSWC-HD-0393-25, June 1995.
13. Nigon, R., "Radio Controlled Model Fluid Research Capabilities," NSWC Research & Development Report, CRDKNSWC-HD-0386-137, January 1994.
14. Park, J., Cutbirth, J. and Brewer, W., "Hydrodynamic Performance of the Large Cavitation Channel (LCC)," Proceedings of FEDSM'03, 4th ASME_JSME Joint Fluids Engineering Conference, Honolulu, HI, July 2003. To appear in J. Fluids Engr.
15. Spina, J. and Meyer, D., "Large-scale Vehicles: An Essential Element in Submarine Technology Insertion," Naval Surface Warfare Center, Carderock Division, Technical Digest, 2001, pp. 1-5.
16. Gertler, M. and Hagen, G., "Standard Equations of Motion for Submarine Simulation," NSWC Research & Development Report, NSRDC 2510, June 1967.
17. Feldman, J., "DTNSRDC Revised Standard Submarine Equations of Motion," NSWC Research & Development Report, DTNSRDC SPD-0393-09, June 1979.
18. Fossen, T. Guidance and Control of Ocean Vehicles, Wiley, NY, 1994.
19. Goldberg, L., "Intact Stability," Principles of Naval Architecture, Second Revision, Edward Lewis, ed., SNAME, NJ, Volume 1, 1988, pp. 63-69.

20. Feldman, J., Naval Surface Warfare Center, Code 5600, private communication.

21. Design of a High-Speed Drag Reduction Experiment, BAA 02-014 (now closed), Office of Naval Research, Dr. L. Patrick Purtell, Technical Point of Contact, June 2002.

22. Wilson, M.B. and Von Kerczek, C., "An Inventory of Some Force Producers for Use in Marine Vehicle Control," NSWC Research & Development Report, DTNSRDC-79/097, Nov 1979, pp. 1-414.

23. Joslin, R. D., Overview of Laminar Flow Control. NASA/TP-1998-208705, October 1998.

24. Joslin, R. D., Aircraft Laminar Flow Control, Annual Review of Fluid Mechanics, Vol. 30, 1998, 1-29.

25. Lauchle, G. C., Eisenhuth, J. J., and Gurney, G. B., Boundary-Layer Transition on a Body of Revolution, Journal of Hydronautics, Vol. 14, No. 4, October 1980, pp. 117-121.

26. Lauchle, G. C. and Gurney, G. B., Laminar Boundary Layer Transition on a Heated Underwater Body, Journal of Fluid Mechanics, Vol. 144, 1984, pp. 79-101.

27. Hansen, R. J. and Hoyt, J. G., Laminar-to-Turbulent Transition on a Body of Revolution with an Extended Favorable Pressure Gradient Forebody, Journal of Fluids Engineering, Vol. 106, June 1984, pp. 202-210.

28. Strazisar, A. J., Reshotko, E., and Prahl, J. M., Experimental Study of the Stability of Heated Laminar Boundary Layers in Water, Journal of Fluid Mechanics, Vol. 83, Part 2, 1977, pp. 225-247.

29. Virk, P. S., Wagger, D. L., and Koury, E, The Asymptotic Maximum Drag Reduction Induced by Additives in Internal Flows, ASME FED-Vol. 237, 1996, pp. 261-276.

30. Hoyer, K. W. and Gyr, A., Heterogeneous Drag Reduction Concepts and Consequences, ASME FED-Vol. 237, 1996, pp. 151-158.

31. Virk, P. S., Drag Reduction Fundamentals, AIChe Journal, Vol. 21, July 1975, pp. 625-656.

32. Virk, P. S., Mickley, H. S., and Smith, K. A., The Ultimate Asymptote and Mean Flow Structure in Toms' Phenomena, Journal of Applied Mechanics, Transaction of ASME, Paper No. 70-APM-HH, 1970.

33. Latorre, R. and Babenko, V. V., Role of Bubble Injection Technique Drag Reduction, Proceedings of the International Symposium on Seawater Drag Reduction, July 22-23, 1998, Newport, RI, pp. 319-325.

34. Meng, J. C. S. and Uhlman, J. S., Jr., Microbubble Formation and Splitting in a Turbulent Boundary Layer for Turbulence Reduction, Proceedings of the International Symposium on Seawater Drag Reduction, July 22-23, 1998, Newport, RI, pp. 341-355.

35. Madavan, N. K., Deutsch, S., and Merkle, C. L., The Effect of Porous Material on Microbubble Skin Friction Reduction, AIAA Paper 84-0348, January 1984.

36. Fontaine, A. and Deutsch, S., "The Influence of the Type of Gas on the Reduction of Skin Friction Drag by Microbubble Injection," Expt. Fluids 13, 1992, pp. 128-136.

37. Xu, J., Maxey, M. and Karniadakis, G., "Numerical Simulation of Turbulent Drag Reduction using Micro-Bubbles," Submitted to Journal of Fluid Mechanics, June 2002.

38. Merkle, C. and Deutsch, S., "Microbubble Drag Reduction in Liquid Turbulent Boundary Layers," Applied Mechanics Reviews 45, 1992, p.121.

39. Loth, E., Univ. of Illinois at Urbana-Champaign, private communication.

40. Choi, B., Ma, M., White, C. and Liu, C., "Electrolytic and Thermal Bubble Generation Using AC Inductive Powering," International Conference on Solid-State Sensors and Actuators (Transducer'99), Sendai, Japan, 7-10 June 1999.

41. Felton, K. and Loth E. "Concentration Distribution of Spherical Bubbles in a Turbulent Boundary Layer," ASME Summer Fluids Engineering Meeting, San Francisco, CA, July 1999, FEDSM99-7360.

42. Kodama, Y., Kakugawa, A., Takahashi, T., Nagaya, S. and Sugiyama, K., "Microbubbles: Drag Reduction Mechanism and Applicability to Ships," 24th Symposium on Naval Hydrodynamics, Fukuoka, Japan, 8-13 July, 2002.

43. Choi, K.-S. and Clayton, B. R., The Mechanism of Turbulent Drag Reduction with Wall Oscillation, Proceedings of the International Symposium on Seawater Drag Reduction, July 22-23, 1998, Newport, RI, pp. 229-235.

44. Choi, K.-S., DeBisschop, J.-R. and Clayton, B.R., "Turbulent Boundary Layer Control by Means of Spanwise Wall Oscillation," AIAA Journal, Vol. 36, No. 7, July 1998, pp. 1157-1163.

45. Dhanak, M. R. and Si, C., On the Physics of Skin Friction Reduction through Wall Oscillation, Proceedings of the International Symposium on Seawater Drag Reduction, July 22-23, 1998, Newport, RI, pp. 237-239.

46. Tardu, S., Local Oscillating Blowing in a Turbulent Boundary Layer, Proceedings of the International Symposium on Seawater Drag Reduction, July 22-23, 1998, Newport, RI, 241-248.

47. Bandyopadhyay, P.R., Castano, J.M., Nedderman, W.H., Thivierge, D.P., Stupak, J., and Fredette, A.R., "Electromagnetic Turbulence Control: Salt Water Experiments on an Axisymmetric Body," Naval Undersea Warfare Center, Newport, RI, NUWC-NPT TR 11,317, October 15, 2001.

48. Ritchie, W., "Experimental Researches in Voltaic and Electromagnetism," Philosophical Transactions of the Royal Society, Vol.122, 1832, pp.279-298.

49. Berger, T.W., Kim, J., Lee, C. and Lim, J., "Turbulent Boundary Layer Control Utilizing the Lorentz Force," Phys. Fluids 12, March 2000, pp. 631-649.

50. Park, J., Henoch, C. and Breuer, K., "Drag Reduction in Turbulent Flows using Lorentz Force Actuation," IUTAM Symposium on Reynolds Number Scaling in Turbulence, Kluwer Academic Publishers, Princeton, NJ, Sept. 11-13, 2002.

51. Park, J., Henoch, C. and Breuer, K., "Lorentz Force Actuators for Wall-Based Flow Control," Expt. Fluids, submitted.

52. Jaskolski, C., "Experimental Implementation of Lorentz Force Actuators for Hydrodynamic Drag Reduction," Master of Science Dissertation, Dept. of Elect. Engr. and Comp. Sci., (C. Chryssostomidis, Ocean Engr., Thesis Supervisor), MIT, May 2002.

53. Du, Y. and Karniadakis, G., "Suppressing Wall Turbulence by means of a Transverse Traveling Wave," Science 288, May 2000, pp. 1230-34.

54. Du, Y., Symeonidis, V. and Karniadakis, G., "Drag Reduction in Wall-Bounded Turbulence via a Transverse Traveling Wave, J. Fluid Mech. 457, 2000, pp.1-34.

55. Karniadakis, G. and Choi, K-S., "Mechanisms on Transverse Motions in Turbulent Wall Flows," Annu. Rev. Fluid Mech. 35, 2003, pp. 45-62.

56. Gray, J., Studies in Animal Locomotion VI: The Propulsive Power of the Dolphin, Journal of Experimental Biology, Vol. 13, 1936, pp. 192-199.

57. Fein, J. A., Dolphin Drag Reduction: Myth or Magic?, Proceedings of the International Symposium on Seawater Drag Reduction, 22-23 July 1998, Newport, RI, pp. 429-432.

58. Carpenter, P.W., and Garrad, A.D., The Hydrodynamic Stability of Flow over Kramer-Type Compliant Surfaces: Part 1. Tollmien Schlichting Instabilities, Journal of Fluid Mechanics, Vol. 155, 1985, pp. 465-510.

59. Carpenter, P.W., and Garrad, A.D., The Hydrodynamic Stability of Flow over Kramer-Type Compliant Surfaces: Part 2. Flow-Induced Surface Instabilities. Journal of Fluid Mechanics, Vol. 170, 1986, pp. 199-232.

60. Willis, G.J.K., Hydrodynamic Stability of Boundary Layers over Compliant Surfaces, Ph.D. Thesis, University of Exeter, 1986.

61. Gaster, M., Is the Dolphin a Red Herring?, Turbulence Management and Relaminarisation, 1988, pp. 285-304, (ed. H.W. Liepmann and R. Narasimha), IUTAM: Bangalore, India.

62. Carpenter, P. W., Optimization of Multiple-Panel Compliant Walls for Delay of Laminar-Turbulent Transition, AIAA Journal, Vol. 31, 1993, pp. 1187-1188.

63. Carpenter, P.W., Lucey, A.D. and Davies, C., "Progress on the Use of Compliant Walls for Laminar-Flow Control," Journal of Aircraft, Vol. 38, No. 3, May-June 2001, pp. 504-511.

64. Bushnell, D.M., NASA Research on Viscous Drag Reduction, II. Laminar-Turbulent Boundary Layers, Vol. 11, 1984, pp. 93-98.

65. Reischman, M.M., A Review of Compliant Coating Drag Reduction Research at ONR, Laminar-Turbulent Boundary Layers, Vol. 11, 1984, pp. 99-105.

66. Duncan, J. H., The Response of an Incompressible, Viscoelastic Coating to Pressure Fluctuations in a Turbulent Boundary Layer, Journal of Fluid Mechanics, Vol. 171, October 1986, pp. 339-363.

67. Gad-el-Hak, M., Compliant Coatings Research: A Guide to the Experimentalist, Journal of Fluids and Structures, Vol. 1, 1987, pp. 55-70.

68. Hess, D., "An Experimental Investigation of a Compliant Surface beneath a Turbulent Boundary Layer," Ph.D. Dissertation, The Johns Hopkins University, Baltimore, MD, September 1990.

69. Hess, D., "Recent Velocity and Displacement Measurements Detailing the Interaction of a Passive Compliant Surface and a Turbulent Boundary Layer," Forum on Turbulent Flows, Fluids Engineering Conference, American Society of Mechanical Engineers, Washington, D.C., FED -155, 29-35, June 20-24, 1993.

70. Hess, D., "An Investigation of Near-Wall Events Interacting with a Passive Compliant Boundary by means of VITA and UV-quadrant Analysis Techniques," Symposium on Flow Noise Modeling, Measurement and Control, Winter Annual Meeting, American Society of Mechanical Engineers, New Orleans, LA, NCA - 15, FED - 168, 75-87, November 28- December 3, 1993.

71. Hess, D., Peattie, R. and Schwarz, W., "A Non-invasive Method for the Measurement of Flow-induced Surface Displacement of a Compliant Surface," *Experiments in Fluids*, **14**, 78-84, 1993.

72. Blackwelder, R. and Kaplan, R., "On the Wall Structure of the Turbulent Boundary Layer," Journal of Fluid Mechanics, **76**, 89-112, 1976.

73. Rathnasingham, R. and Breuer, K., "System Identification and Control of a Turbulent Boundary Layer," Physics of Fluids 9, July 1997, pp. 1867-69.

74. Rathnasingham, R. and Breuer, K., "Feedforward Control of Turbulent Boundary Layers," Submitted to Journal of Fluid Mechanics, February 2003.

75. Walsh, M. J., Drag Characteristics of V-Groove and Transverse Curvature Riblets, Progress in Astronautics and Aeronautics, AIAA Viscous Flow Drag Reduction, Vol. 72, 1980, (ed. Gary R. Hough), pp. 169-184.

76. Walsh, M. J., Turbulent Boundary Layer Drag Reduction Using Riblets, AIAA Paper 82-0169, January 1982.

77. Walsh, M. J. and Lindemann, A. M., Optimization and Application of Riblets for Turbulent Drag Reduction, AIAA Paper 84-0347, January 1984.

78. Gallagher, J. A. and Thomas, A. S. W., Turbulent Boundary Layer Characteristics over Streamwise Grooves, AIAA Paper 84-2185, August 1984.

79. Anders, J. B., Walsh, M. J. and Bushnell, D. M., The Fix for Tough Spots, Aerospace America, January 1988, pp. 14.

80. DeMeis, R., Stick-to-it Riblets. Aerospace America, January 1988, pp. 48-49.

81. Calarese, W., Crisler, W. P., and Gustafson, G. L., Afterbody Drag Reduction by Vortex Generators, AIAA Paper 85-0354, January 1985.

82. Wortman, A., Alleviation of Fuselage Form Drag using Vortex Flows, US Department of Energy Report DOE/CE/15277-T1, September 1987.

83. Lin, J. C., Control of Turbulent Boundary-Layer Separation using Micro-Vortex Generators, AIAA Paper 99-3404, June 1999.

84. Lin, J. C., Robinson, S. K., McGhee, R. J., and Valarezo, W. O., Separation Control on High-Lift Airfoils via Micro-Vortex Generators, Journal of Aircraft, Vol. 31, No. 6, 1994, pp. 1317-1323.

85. Lin, J., Sedler, T., Stiver, D., Faller, W. and Hess, D., "Application of Micro-Vortex Generators for Submarine Maneuvering Enhancement," International Symposium on Seawater Drag Reduction, NUWC, Newport, RI, July 22-24, 1998.

86. Bender, E. E., Anderson, B. H., and Yagle, P. J., Vortex Generator Modeling for Navier-Stokes Codes, ASME Paper FEDSM99-6919, July 1999.

87. Wetzel, T. G. and Simpson, R. L., Effects of Fin and Jet Vortex Generators on the Crossflow, Journal of Aircraft, Vol. 35, No. 3, May-June 1998, pp. 370-379.

88. McManus, K. and Magill, J., Separation Control in Incompressible and Compressible Flows using Pulsed Jets, AIAA Paper 96-1948, June 1996.

89. Ingard, U. and Labate, S., Acoustic Circulation Effects and the Nonlinear Impedance of Orifices, Journal of the Acoustical Society of America, Vol. 22, No. 2, March 1950, pp. 211-218.

90. Wiltse, J. M. and Glezer, A., Manipulation of Free Shear Flows Using Piezoelectric Actuators, Journal of Fluid Mechanics, Vol. 249, 1993, 261-285.

91. Smith, B. L. and Glezer, A., The Formation and Evolution of Synthetic Jets, Physics of Fluids, Vol. 10, No. 9, September 1998, pp. 2281-2297.

92. Glezer, A. and Amitay, M., "Synthetic Jets," Annual Review of Fluid Mechanics, Vol. 34, 2002, pp. 503-529.

93. Bryant, R. G., Fox, R. L., Lachowicz, J. T., and Chen, F.-J., Piezoelectric Synthetic Jets for Aircraft Control Surfaces, Smart Structures and Materials 6th Annual International Symposium, Newport Beach, CA, March 1-5, 1999.

94. Cattafesta, L., Mathew, J., Wang, W. and Kurdila, A., Modeling of Piezoelectric Actuators for Fluid Flow Control, SAE Paper 2000-01-5534.

95. Burr, R. F., Berger, S. S., and Tence, D. A., Overview of Phase Change Piezoelectric Ink Jet Fluids Modeling and Design, ASME FED-Vol. 239, 1996, pp. 545-552.

96. Seifert, A., Eliahu, S., Greenblatt, D. and Wygnanski, I., Use of Piezoelectric Actuators for Airfoil Separation Control, AIAA Journal, Vol. 36, No. 8, 1998, pp. 1535-1537.

97. Hsiao, F.-B., Wang, T.-Z., and Zohar, Y., Flow Separation Control of a 2-D Airfoil by a Leading-Edge Oscillating Flap, Pacific International Conference on Aerospace Science and Technology, Vol. 1, 1993, pp. 250-256.

98. Seifert, A., Bachar, T., Koss, D., Shepshelovich, M., and Wygnanski, I., Oscillatory Blowing: A Tool to Delay Boundary-Layer Separation, AIAA Journal, Vol. 31, No. 11, November 1993, pp. 2052-2060.

99. Seifert, A., Darabi, A., and Wygnanski, I., Delay of Airfoil Stall by Periodic Excitation, Journal of Aircraft, Vol. 33, No. 4, July-August 1996, pp. 691-698.

100. Seifert, A., Bachar, T., Wygnanski, I., Kariv, A., Cohen, H., and Yoeli, R., Application of Active Separation Control to a Small Unmanned Air Vehicle, Journal of Aircraft, Vol. 36, No. 2, 1998, pp. 474-477.

101. Seifert, A. and Pack, L. G., Oscillatory Excitation of Unsteady Compressible Flows over Airfoils at Flight Reynolds Numbers, 37th AIAA Aerospace Sciences Meeting & Exhibit, Reno, NV, January 11-14, 1999. AIAA Paper 99-0925, January 1999.

102. Seifert, A. and Pack, L. G., Oscillatory Control of Separation at High Reynolds Numbers, AIAA Journal, Vol. 33, No. 9, 1999, pp. 1062-1071.

103. Davidson, I.M., "Aerofoil Boundary Layer Control System", British Patent No 913754, 1960.

104. Kind, R.J. and Maull, D.J., "An Experimental Investigation of a Low-Speed Circulation Controlled Airfoil," Aeronautical Quarterly, Vol. 19, pp 170-182, May 1968.

105. Cheeseman, I.C. and Read, A.R., "The Application of Circulation Control by Blowing to Helicopter Rotors," J.R.AE.S., Vol. 71, No. 848 , Jul 1966.

106. Englar, R.J., and Applegate, C.A., Circulation Control – A Bibliography of DTNSDRC Research and Selected Outside References, DTNSDRC Report 84-052, October 1984.

107. Ambrosiani, J.P. and Ness, N., "Analysis of a Circulation Controlled Elliptical Airfoil," West Virginia University TR-30, April 1971.

108. Roberts, S.C., "WVU Circulation Controlled STOL Aircraft Flight Tests," West Virginia University TR-42, July 1974.

109. Lee, D.G., Talley, E.W. and Davidson, Jr., H.D., "The Applicability of Rotating Cylinders as a Control Mechanism for Submarines," NSWC Research & Development Report, Aviation and Surface Effects Department, ASED-298, Aug 1973, pp. 1-15.

110. Pugliese, A.J., and Englar, R.J., Flight Testing the Circulation Control Wing, AIAA Paper 79-1791, August 1979.

111. Novak, C. J., Cornelius, K. C., and Roads, R. K., Experimental Investigations of the Circular Wall Jet on a Circulation Control Airfoil, AIAA Paper 87-0155, January 1987.

112. Englar, R.J., and Applegate, C.A., Circulation Control – A Bibliography of DTNSDRC Research and Selected Outside References, DTNSDRC Report 84-052, October 1984.

113. Englar, R.J. (GTRI), "Circulation Control Pneumatic Aerodynamics: Blown Force and Moment Augmentation and Modification; Past, Present & Future," Fluids 2000, June 2000, AIAA 2000-2541.

114. Oyler, T. E. and Palmer, W. E., Exploratory Investigation of Pulse Blowing for Boundary Layer Control. North American Rockwell Corp., Report No. NR 72H-12, January 1972.

115. Morger, K.M. and Clark, D.R., "Analytic and Experimental Verification of the NOTAR Circulation Control Tail Boom," American Helicopter Society, 40th Annual Forum, May 1984.

116. Brand, A.G., et al. (Bell Helicopter), "Analysis, Design, and Testing of the Coanda Effect Exhaust Deflector of the V-22 Tiltrotor," Twentieth European Rotorcraft Forum, Paper 15, Oct 1994.

117. Ham, N.D. et al., "Wind Tunnel Generation of Sinusoidal Lateral and Longitudinal Gusts by Circulation of Twin Parallel Airfoils," MIT ASRL-TR-174-3, NASA-CR-**137547,** Aug 1974.

118. Newman, B., "The Deflexion of Plane Jets by Adjacent Boundaries – Coanda Effect," in Boundary Layer and Flow Control, Vol. 1, G. Lachman, ed., Pergamon Press, 1961, pp 232-264.

119. Abramson, J., "The Low Speed Characteristics of a 15-Percent Quasi-Elliptical Circulation Control Airfoil with Distributed Camber," DTNSRDC/ASED-79/07, May 1979.

120. Rogers, E., Naval Surface Warfare Center, Code 5300, private communication.

121. Abramson, J. and Rogers, E.O., "High Speed Characteristics of Circulation Control Airfoils," AIAA Paper 83-0265, January 1983.

122. Howe, M.S., "Analytical Study of the Noise Generated by a Coanda Wall Jet Circulation Control Device," Boston University AM-00-004, Oct 2000.

123. Ericsson, L. E. and Beyers, M. E., Effect of Nose Slenderness on Forebody Flow Control, Journal of Aircraft, Vol. 36, No. 5, September-October 1999, pp. 885-889.

124. Ffowcs-Williams, J. E., and Zhao, B. C., The Active Control of Vortex Shedding, Journal of Fluids and Structures, Vol. 3, 1989, pp. 115-122.

125. Tokumaru, P. T. and Dimotakis, P. E., Rotary Oscillation Control of a Cylinder Wake, Journal of Fluid Mechanics, Vol. 224, 1991, pp. 77-90.

126. Nguyen, T., Bochinski, D. and Gowing, S., "Tab Assisted Control Surface for Submarine Application," Royal Institute of Naval Architects International Symposium, Warship '99:Naval Submarines **6**, London, UK, 1999.

127. Sung, C. and Rhee, B., "Prediction of Forces and Moments of Rudders with Flap and Tab," Seventh International Conference on Numerical Ship Hydrodynamics, Nantes, France, July 19-22, 1999.

128. Sung, C., Rhee, B. and Koh, I., "Validation of Tab Assisted Control Surface Computation," 23rd Symposium on Naval Hydrodynamics, Val de Reuil, France, September 17-22, 2000.

129. Gowing, S., Carpenter, B., Atsavapranee, P., Lee, Y., Lee, M. and Hess, D., "FlexTAC: Flexible Tab Assisted Control for Submarine Application," NSWC Research & Development Report, NSWCCD-50-TR-2003/029, June 2003.

130. Lee, Y., Ebert, M. and Hosangadi, A., "Flow Predictions for Multi-Element Control Surfaces," NSWC Research & Development Report, NSWCCD-50-TR-2002/061, December 2002.

131. Quackenbush, T., Bilanin, A., Batcho, P., McKillip, R. and Carpenter, B., "Implementation of Vortex Wake Control Using SMA-actuated Devices", Proc. of SPIE Smart Structures and Materials 1997, Industrial and Commercial Applications of Smart Structures Technologies, Vol. 3044, J. Sater ed., San Diego CA, pp.114-122, March 2-6, 1997.

132. Quackenbush, T.R., et al.: "Design, Fabrication and Test Planning for an SMA-Actuated Vortex Wake Control System", Proc. of SPIE Smart Structures and Materials 1998, Industrial and Commercial Applications of Smart Structures Technologies, Burrows ed., San Diego CA, March 1998.

133. Quackenbush, T.R., et al.: "Test Results for an SMA-Actuated Vortex Wake Control System," Proc. of SPIE Smart Structures

and Materials 1999, Industrial and Commercial Applications of Smart Structures Technologies, Jacobs ed., San Diego CA, March 1999.

134. Quackenbush, T.R., et al., http://www.darpa.mil/dso/thrust/matdev/smartmat/Programs/vortex.html

135. Gilyard, G. B. and Bolonkin, A., Optimal Pitch Thrust-Vector Angle and Benefits for all Flight Regimes, NASA TM-2000-209021, March 2000.

136. Bowers, A. H. and Pahle, J. W., Thrust Vectoring on the NASA F-18 High Alpha Research Vehicle, NASA TM 4771, November 1996.

137. Pack, L. G. and Seifert, A., Periodic Excitation for Jet Vectoring and Enhanced Spreading, 37th AIAA Aerospace Sciences Meeting & Exhibit, Reno, NV, AIAA Paper 99-0672, January 11-14, 1999.

138. Quackenbush, T., Continuum Dynamics, Inc., http://www.continuum-dynamics.com/ Technical Point of Contact, private communication.

139. Roddy, R., "Investigation of the Resistance, Propulsion, Stability and Control Characteristics of the NUWC/ARL UUV IMP from Captive Model Experiments," NSWC Research & Development Report, NSWCCD-50-TR-2003/010, March 2003.

140. Seifert, A., Theofilis, T. and Joslin, R.D., "Issues in Active Flow Control: Theory, Simulation and Experiment," 1st AIAA Flow Control Conference, St. Louis, MO, June 24-26, 2002, AIAA 2002-3277, pp.1-41.

141. Gad-el-Hak, M., "Flow Control: The Future," Journal of Aircraft, Vol. 38, No. 3, May-June 2001, pp. 402-418.

142. Journal of Aircraft, Vol. 38, No. 3, May-June 2001.

143. McMichael, J., "Active Flow Control — Bright Prospects and Basic Challenges," correction in Journal of Aircraft, Vol. 38, No. 4, July-August 2001, pp.783-784.

144. Koumoutsakos, P., Bewley, T. R., Hammond, E. P., and Moin, P., "Feedback Algorithms for Turbulence Control-Some Recent Developments," AIAA Paper 97-2008, Jun. 1997.

145. Gunzburger, M. D. (ed) Flow Control, Springer-Verlag, New York, 1995.

146. Borggaard, J., Burkardt, J., Gunzburger, M., and Peterson, J., Optimal Design and Control, Birkhauser, Boston, 1995.

147. Gruver, W. A. and Sachs, E, Algorithmic Methods in Optimal Control, Pitman Advanced Publishing, Boston, 1980, 233 pp.

148. Burghes, D. N. and Graham, A., Introduction to Control Theory, Including Optimal Control, John Wiley and Sons, New York, 1980.

149. Joslin, R.D., Gunzburger, M.D., Nicolaides, R.A., Erlebacher, G. and Hussaini, M.Y., "Self-Contained Automated Methodology for Optimal Flow Control," AIAA Journal, Vol. 35, No. 5, 1997, pp. 816-824.

150. Joslin, R. D., Gunzburger, M. D., Nicolaides, R.A., Erlebacher, G. and Hussaini, M. Y., "A Self-Contained, Automated Methodology for Optimal Flow Control Validated for Transition Delay," NASA CR 198215, 1995.

151. Bewley, T. R., Moin, P., and Teman, R., "Optimal and Robust Approaches for Linear and Nonlinear Regulation Problems in Fluid Mechanics," AIAA Paper 97-1872, Jun. 1997.

152. Bewley, T. R., "Flow Control: New Challenges for a New Renaissance," Progress in Aerospace Sciences, Vol. 37, 2001, pp. 21-58.

153. He, J.-W., Glowinski, R., Metcalfe, R., Nordlander, A. and Periaux, J., "Active Control and Drag Optimization for Flow Past a Circular Cylinder," Journal of Computational Physics 163, 2000, pp. 83-117.

154. Walther, S., Airiau, C. and Bottaro, A., "Optimal Control of Tollmien-Schlichting Waves in a Developing Boundary Layer," Physics of Fluids, Vol. 13, No. 7, July 2001, pp. 2087-2096.

155. Airiau, C., Bottaro, A., Walther, S. and Legendre, D., "A Methodology for Optimal Laminar Flow Control: Application to the Damping of Tollmien-Schlichting Waves in a Boundary Layer," Physics of Fluids, Vol. 15, No. 5, May 2003, pp. 1131-1145.

156. Hinze, M. and Kunisch, K., "Second Order Methods for Optimal Control of Time-Dependent Fluid Flow," SIAM Journal on Control and Optimization, Vol. 40, No. 3, 2002, pp. 925-946.

157. Choi, H., Temam, R., Moin, P. and Kim, J., "Feedback Control for Unsteady Flow and its Application to the Stochastic Burgers Equation," Journal of Fluid Mechanics, Vol. 253, 1993, pp. 509-543.

158. Breuer, K.S., "Active Control of Wall Pressure Fluctuations in a Turbulent Boundary Layer," Symposium on Flow Noise Modeling, Measurement and Control, Winter Annual Meeting, American Society of Mechanical Engineers, New Orleans, LA, NCA - 15, FED - 168, Nov 28- Dec 3, 1993, pp. 39-47.

159. Choi, H., Moin, P. and Kim, J., "Active Turbulence Control for Drag Reduction in Wall-Bounded Flows," Journal of Fluid Mechanics, Vol. 262, 1994, pp. 75-110.

160. Rathnasingham, R. and Breuer, K.S., "System Identification and Control of a Turbulent Boundary Layer," Physics of Fluids, Vol. 9, No. 7, July 1997, pp. 1867-1869.

161. Rathnasingham, R. and Breuer, K.S., Feedforward Control of Turbulent Boundary Layers," submitted to Journal of Fluid Mechanics, Feb 2003.

162. Tsao, T., Jiang, F., Miller, R., Tai, Y.-C., Gupta, B., Goodman, R., Tung, S. and Ho, C.-M., "An Integrated MEMS System for Turbulent Boundary Layer Control," Technical Digest, 1997 International Conference on Solid-State Sensors and Actuators (Transducers '97), Chicago, IL, June 16-19, 1997, Vol. 1, pp. 315-318.

163. Joslin, R.D., Nicolaides, R.A., Erlebacher, G., Hussaini, M.Y. and Gunzburger, M.D., "Active Control of Boundary Layer Instabilities: Use of Sensors and Spectral Controller," AIAA Journal, Vol. 33, No. 8, Aug 1995, pp. 1521-1523.

164. Koumoutsakos, P., "Vorticity Flux Control for a Turbulent Channel Flow," Physics of Fluids Vol. 11, No. 2, Feb 1999, pp. 248-250.

165. Schoppa, W. and Hussain, F. "A Large-Scale Control Strategy for Drag Reduction in Turbulent Boundary layers," Physics of Fluids, Vol. 10, No. 3, May 1998, pp. 1049-1051.

166. Lee, C., Kim, J., Babcock, D. and Goodman, R., "Application of Neural Networks to Turbulence Control for Drag Reduction," Physics of Fluids, Vol. 9, No. 6, June 1997, pp. 1740-1747.

167. Tardu, S., "Active Control of Near-Wall Turbulence by Local Oscillating Blowing," Journal of Fluid Mechanics, Vol. 439, 2001, pp. 217-253.

168. Lee, C., Kim, J. and Choi, H., "Suboptimal Control of Turbulent Channel Flow for Drag Reduction," Journal of Fluid Mechanics, Vol. 358, 1998, pp. 245-258.

169. Bewley, T.R., Moin, P. and Temam, R., "DNS-Based Predictive Control of Turbulence: An Optimal Benchmark for feedback algorithms," Journal of Fluid Mechanics, Vol. 447, 2001, pp. 179-225.

170. Cattafesta III, L.N., Garg, S. and Shukla, D., "Development of Piezoelectric Actuators for Active Flow Control," AIAA Journal Vol. 39, No. 8, Aug 2001, pp. 1562-1568.

171. Jacobson, S.A. and Reynolds, W.A., "Active Control of Streamwise Vortices and Streaks in Boundary Layers," Journal of Fluid Mechanics, Vol. 360, 1998, pp. 179-211.

172. Greenblatt, D. and Wygnanski, I.J., "The Control of Flow Separation by Periodic Excitation," Progress in Aerospace Sciences, Vol. 36, 2000, pp. 487-545.

173. Greenblatt, D. and Wygnanski, I., "Dynamic Stall Control by Periodic Excitation, Part 1: NACA 0015 Parametric Study," Journal of Aircraft, Vol. 38, No. 3, May-June 2001, pp. 430-438.

174. Greenblatt, D., Nishri, B., Darabi, A. and Wygnanski, I., "Dynamic Stall Control by Periodic Excitation, Part 2: Mechanisms," Journal of Aircraft, Vol. 38, No. 3, May-June 2001, pp. 439-447.

175. Faller, W., Schreck, S. and Luttges, M., "Neural Network Prediction and Control of Three-Dimensional Unsteady Separated Flow Fields," Journal of Aircraft, Vol. 32, No. 6, Dec 1995, pp. 1213-1220.

176. Faller, W.E. and Schreck, S.J., "Unsteady Fluid Mechanics Applications of Neural Networks," Journal of Aircraft, Vol. 34, No. 1, Jan-Feb 1997, pp. 48-55.

177. Louie, L., Fry, D. and Jessup, S., "An Active Control System to Cancel Unsteady Foil Forces," Proceedings of the ASME Winter Annual Meeting, Chicago, IL Nov 1994.

178. Fry, D.J., Louie, L.L., and Jessup, S., "A Water Tunnel Evaluation of a Novel Actuator and Active Control System to Cancel Unsteady Foil Forces," NSWC Research & Development Report, CDNSWC/SHD-1401-04, December 1993.

179. Fry, D.J. and McGuigan, S., "Hydrofoil Circulation Control via a Miniature Valve for Alternating Flows between Two Exit Slots," NSWC Research & Development Report, CDNSWC/SHD-1401-02, December 1993.

180. Yang, J., Ghia, K.N., Ghia, U. and Osswald, G.A., "Management of Dynamic Stall Phenomenon through Active Control of Unsteady Separation," AIAA Shear Flow Conference, Orlando, FL, July 6-9, 1993, AIAA-93-3284, pp. 1-18.

181. Seifert, A. and Pack, L.G., "Effects of Sweep on Active Separation Control at High Reynolds Numbers," Journal of Aircraft, Vol. 40, No. 1, Jan-Feb 2003, pp. 120-126.

182. Katz, Y., Nishri, B. and Wygnanski, I., "The Delay of Turbulent Boundary Layer Separation by Oscillatory Active Control," Physics of Fluids A, Vol. 1, No. 2, Feb 1989, pp. 179-181.

183. Sinha, S.K., "Flow Separation Control with Microflexural Wall Vibrations," Journal of Aircraft, Vol. 38, No. 3, May-June 2001, pp. 496-503.

184. Kiya, M., Mochizuki, O. and Ishikawa, H., "Interaction between Vortex Rings and a Separated Shear Layer: Towards Active Control of Separation Zones," Journal of Fluids and Structures, Vol. 15, 2001, pp. 399-413.

185. Fu, T.C., Atsavapranee, P. and Hess, D.E., "PIV Measurements of the Cross-Flow Wake of a Turning Submarine Model (ONR Body-1)," Proceedings of the 24th Symposium on Naval Hydrodynamics, Fukuoka, Japan, July 8-13, 2002, pp. 154-166.

186. Fu, T.C., Atsavapranee, P. and Hess, D.E., "PIV Measurements of the Cross-Flow Velocity Field around a Turning Submarine Model (ONR Body-1), Part 1: Experimental Setup," NSWC Research & Development Report, NSWCCD-50-TR-2002/019, Feb 2002.

187. Sung, C.-H., Jiang, M.-Y., Rhee, B., Percival, S., Atsavapranee, P. and Koh, I.-Y., "Validation of the Flow around a Turning Submarine," Proceedings of the 24th Symposium on Naval Hydrodynamics, Fukuoka, Japan, July 8-13, 2002, pp. 167-178.

188. Gibson, J.D., Ammeen, E.S. and Feldman, J.P., "A Brief History of Linear Quadratic Gaussian Control of Submarines at MIT with an Introduction to LQG/LTR Design," Proceedings of the ASNE Intelligent Ship Symposium V, Philadelphia, PA, 12-13 May 2003.

189. Ammeen, E. and Faller, W., "Submarine Advanced Control and Monitoring," ASNE Intelligent Ship Symposium IV, 2-3 April 2001.

190. Ammeen, E.S. and Beale, G.O., "Advanced Control and Monitoring: Improving Marine Vehicle Safety and Performance," 13th International Ship Control Systems Symposium, Orlando, FL, 7-9 April 2003.

191. Hammett, R., Coakley, M., Sevigny, D. and Zamojski, R., "Automatic Performance Monitoring Enhances Seawolf Submarine Ship Control Maintainability," Naval Engineers Journal, Vol. 110, No. 2, Mar 1998, pp. 49-59.

192. Mendel, J.M., "Fuzzy Logic Systems for Engineering: A Tutorial," Proceedings of the IEEE, Vol. 83, No. 3, Mar 1995, pp. 345-377.

193. Mendel, J.M., "Correction to Fuzzy Logic Systems for Engineering: A Tutorial," Proceedings of the IEEE, Vol. 83, No. 9, Sept 1995, p. 1293.

194. "Applications of Fuzzy Logic in Control Design," MATLAB Technical Computing Brief, Preprint, The MathWorks, Inc., 1995, pp. 1-9.

195. Takagi, T. and Sugeno, M., "Fuzzy Identification of Systems and Its Applications to Modeling and Control," IEEE Transactions on Systems, Man and Cybernetics, Vol. SMC-15, No. 1, Jan-Feb 1985, pp. 116-132.

196. Mendel, J.M. and Mouzouris, G.C., "Designing Fuzzy Logic Systems," IEEE Transactions on Circuits and Systems – II: Analog and Digital Signal Processing, Vol. 44, No. 11, Nov 1997, pp. 885-895.

197. Mendel, J.M., "Uncertainty, Fuzzy Logic, and Signal Processing," Signal Processing, Vol. 80, 2000, pp. 913-933.

198. Johnston, R., "Fuzzy Logic Control," Microelectronics Journal, Vol. 26, No. 5, 1995, pp. 481-495.

199. Choi, J.L., Lee, D.K. and Kim, H.Y., "The Use of Fuzzy Logic Theory in the Design of a Depth Control System for a Submersible Vehicle," Warship '93, Proceedings of the International Symposium on Naval Submarines, Vol. 4: Boats Weapons and Systems, Paper No. 23, London, UK, 11-13 May 1993.

200. Ammeen, E.S. and Beale, G.O., "Fuzzy Depth Control for a Submersible Vehicle," IEEE International Symposium on Industrial Electronics, Guimaraes, Portugal, July 1997, pp. 1185-1190.

201. Ammeen, E.S. and Beale, G.O., "Fuzzy Control Application to a Submarine Depth Control System," NSWC Research & Development Report, CRDKNSWC-HD-1437-02, Mar 1996, pp. 1-86.

202. Kim, R.R., Ware, J.R. and Ammeen, E.S., "Applications of Neural Networks and Fuzzy Logic in Failure Detection and Fault Tolerant Control System Design," 11th Ship Control Symposium, Southhampton, UK, April 1997.

203. Faller, W., Schreck, S., Helin, H. and Luttges, M., "Real-Time Prediction of Three-Dimensional Dynamic Reattachment Using Neural Networks," Journal of Aircraft, Vol. 32, No. 6, 1995.

204. Faller, W., Smith, W. and Huang, T., "Applied Dynamic System Modeling: Six Degree-Of-Freedom Simulation Of Forced Unsteady Maneuvers Using Recursive Neural Networks," 35th AIAA Aerospace Sciences Meeting, Paper 97-0336, 1997, pp. 1-46.

205. Faller, W., Hess, D., Smith, W. and Huang, T., "Full-Scale Submarine Maneuver Simulation," 1st Symposium on Marine Applications of Computational Fluid Dynamics, U.S. Navy Hydrodynamic / Hydroacoustic Technology Center, McLean, Va., May 1998.

206. Hess, D., Faller, W., Smith, W. and Huang, T., "Neural Networks as Virtual Sensors," 37th AIAA Aerospace Sciences Meeting, Paper 99-0259, 1999, pp. 1-10.

207. Faller, W., Hess, D., Smith, W. and Huang, T., "Applications of Recursive Neural Network Technologies to Hydrodynamics," Proceedings of the Twenty-Second Symposium on Naval Hydrodynamics, Washington, D.C., Vol. 3, August 1998, pp. 1-15.

208. Hess, D., Faller, W., Smith, W. and Huang, T., "Simulation of Ship Tactical Circle Maneuvers Using Recursive Neural Networks," Proceedings of the Workshop on Artificial Intelligence and Optimization for Marine Applications, Hamburg, Germany, September 1998, pp. 19-22.

209. Hess, D. and Faller, W., "Simulation of Ship Maneuvers Using Recursive Neural Networks," Proceedings of the Twenty-Third Symposium on Naval Hydrodynamics, Val de Reuil, France, September 2000.

210. Faller, W., "Recursive Neural Networks: Toward Advances in Simulation and Control," AIAA Fluids 2000, Paper 2000-2470, June 19-22, 2000, pp.1-9.

211. Hess, D. and Faller, W., "Using Recursive Neural Networks for Blind Predictions of Submarine Maneuvers," Twenty-Fourth Symposium on Naval Hydrodynamics, Fukuoka, Japan, July 8-13, 2002.

212. Atlar, M., Mesbahi, E., Roskilly, A.P. and Gale, M. "Efficient Techniques in Time-Domain Motion Simulation Based on Artificial Neural Network," International Symposium on Ship Motions and Manoeuvrability, RINA, London, U.K., Feb. 1998, pp.1-23.

213. Mesbahi, E. and Atlar, M. "Applications of Artificial Neural Networks in Marine Design and Modeling," Proceedings of the Workshop on Artificial Intelligence and Optimization for Marine Applications, Hamburg, Germany, September 1998, pp. 31-41.

214. Li, D. and Gu, M.X. "Dynamic Positioning of Ships Using a Planned Neural Network Controller," Journal of Ship Research, Vol. 40, No. 2, June 1996, pp.164-171.

215. Burns, R.S. and Polkinghorne, M., "A Neural Network Controller for Optimal Guidance of Surface Ships," 10th Symposium on Ship Control Systems, Ottawa, Canada, 25-29 Oct 1993, Vol. 2, pp. 195-210.

216. Logan, K.P., "Neural Network-Based Autopilot for Improved Ship Control," Proceedings of the ASNE Intelligent Ship Symposium, Philadelphia, PA, 1-2 June 1994.

217. Witt, N.A. and Miller, K.M., "A Neural Network Autopilot for Ship Control," 3rd International Conference on Maritime Communications and Control, Institute of Marine Engineers, London, UK, 7-8 July 1993, Paper 4, pp. 47-59.

218. Sutton, R., Johnson, C. and Roberts, G.N., "Depth Control of an Unmanned Underwater Vehicle Using Neural Networks," Oceans '94, Oceans Engineering for Today's Technology and Tomorrow's Preservation, Vol. 3, Brest, France, 13-16 Sept 1994, pp. 121-125.

219. Norton, M.J., "The Use of a Simple Neural Network in the Motion Control of Unmanned Undersea Vehicles," Proceedings of the 6th International Symposium on Unmanned Untethered Submersible Technology, Durham, NH, 12-14 June 1989, pp. 425-433.

220. Venugopal, K.P., Pandya, A.S. and Sudhakar, R., "Adaptive Neural Network Controllers for Autonomous Underwater Vehicles," Intervention/ROV '91 Conference and Exposition, Hollywood, FL, 21-23 May 1991, 361-366.

221. Mort, N., Derradji, D.A., Tiano, A. and Ranzi, A., "Application of Neural Networks to Marine Vehicle Control," 10th Symposium on Ship Control Systems, Ottawa, Canada, 25-29 Oct 1993, Vol.2, pp. 287-306.

222. Bushnell, D. M., Application Frontiers of "Designer Fluid Mechanics"--Visions versus Reality or An attempt to Answer the Perennial Question "Why Isn't It Used?", AIAA Paper 97-2110, June 1997.